Sleeping ribosomes: bacterial signaling triggers RaiA mediated persistence to aminoglycosides

Manon Lang, Evelyne Krin, Chloé Korlowski, Odile Sismeiro, Hugo Varet, Jean-Yves J.-Y. Coppée, Didier Mazel, Zeynep Baharoglu

Sleeping ribosomes: bacterial signaling triggers RaiA mediated persistence to aminoglycosides.

Manon Lang[1,2], Evelyne Krin[1], Chloé Korlowski[1], Odile Sismeiro[3], Hugo Varet[3,4], Jean-Yves Coppée[3], Didier Mazel[1]*, Zeynep Baharoglu[1]*

[1] Département Génomes et Génétique, Institut Pasteur, UMR3525, CNRS, Unité Plasticité du Génome Bactérien, Paris, France.
[2] Sorbonne Université, Collège Doctoral, F-75005 Paris, France.
[3] Biomics technological plateform, Center for Technological Resources and Research, Institut Pasteur, Paris, France.
[4] Bioinformatics and Biostatistics Hub, Department of Computational Biology, USR 3756 CNRS, Institut Pasteur, Paris, France.

* corresponding authors, mazel@pasteur.fr, zeynep.baharoglu@pasteur.fr

Abstract

Indole is a molecule proposed to be involved in bacterial signaling. We find that indole secretion is induced by sublethal tobramycin concentrations and increases persistence to aminoglycosides in *V. cholerae*. Indole transcriptomics showed increased expression of *raiA*, a ribosome associated factor. Deletion of *raiA* abolishes the appearance of indole dependent persisters to aminoglycosides, while its overexpression leads to 100-fold increase of persisters, and a reduction in lag phase, evocative of increased active 70S ribosome content, confirmed by sucrose gradient analysis. We propose that, under stress conditions, RaiA-bound inactive 70S ribosomes are stored as so-called "sleeping ribosomes", and are rapidly reactivated upon stress relief. Our results point to an active process of persister formation, through ribosome protection during translational stress (e.g. aminoglycoside treatment), and reactivation upon antibiotic removal. Translation is a universal process, and these results could help elucidate a mechanism of persistence formation in a controlled, thus inducible way.

Introduction

Antibiotic resistance is a major public health concern leading to increased health care costs and mortality (Opatowski et al., 2019; Touat et al., 2019). Although the majority of studies address the response of bacteria to lethal doses of antibiotics, the effect of low doses of antibiotics on bacteria has also recently started to draw attention. Antibiotic concentrations lower than the minimal inhibitory concentration (sub-MICs) have historically been proposed to serve as signaling molecules (Davies et al., 2006), provoking considerable changes in transcription and triggering a wide variety of cellular responses in different bacterial species (Andersson and Hughes, 2014) and mutagenesis (Gutierrez et al., 2013). In *V. cholerae*, sub-MIC aminoglycosides (AGs) are known to activate various stress response pathways, such as the SOS (Baharoglu et al., 2014; Baharoglu and Mazel, 2011) and RpoS stress responses (Baharoglu et al., 2013), allowing cells to cope with increased reactive oxygen species (ROS) levels and DNA breaks (Negro et al., 2019). AGs are bactericidal antibiotics that are known to enter the bacterial cell through the proton motive force (Fraimow et al., 1991; Herisse et al., 2017; Taber et al., 1987). AGs target the ribosome, leading to mistranslation and eventually cell death (Davis, 1987).
Interestingly, sub-MIC antibiotics, among which AGs, have been shown to stimulate the production of a small molecule, indole (Han et al., 2011). Indole is a byproduct of tryptophan degradation by tryptophanase TnaA (Evans et al., 1941) in both Gram+ and Gram- bacterial species (Lee and Lee, 2010), together with pyruvate and ammonia. While pyruvate and ammonia are respectively sources of carbon and nitrogen, the role of indole is not well understood. Indole is also found in plants and animals, and was linked with signaling and human diseases (for a review, (Lee et al., 2015)). Common indole concentrations in the human gut are in the order of 250-1100 µM, and up to 200 µM in blood and other tissues. Regulation of indole production has been described, namely through carbon source utilization (Botsford and DeMoss, 1971) and catabolic repression (Yanofsky et al., 1991), amino acid

availability (Newton and Snell, 1965), cold temperature (Lee et al., 2008), heat shock (Li et al., 2003) and growth phase (Kobayashi et al., 2006). Particularly, indole is produced during transition from exponential to stationary phase (Lelong et al., 2007).

In *E. coli*, indole is nontoxic at physiologic concentrations (below 1 mM) (Lee et al., 2007), and does not change the growth rate (Lee et al., 2008). At high concentrations however (above 1-3 mM), indole inhibits cell division (Chant and Summers, 2007; Chimerel et al., 2012). In *V. cholerae*, indole secretion reaches its maximum at 600 µM during transition from midlog to stationary phase (Howard et al., 2019; Mueller et al., 2009) and was not observed to have any effect on the polarity of the *V. cholerae* cell membrane at this concentration (Mueller et al., 2009).

Indole can pass across the cell membrane without the need for a transporter (Pinero-Fernandez et al., 2011), and was proposed to act as an interkingdom signaling molecule (Martino et al., 2003; Wang et al., 2001). An effect of indole in persistence to antibiotics has also been observed. At toxic concentrations (1-2 mM), where indole behaves as a membrane ionophore, it was observed to reduce persistence of stationary phase cultures to tested antibiotics (ciprofloxacin, ampicillin) (Hu et al., 2015). However, studies in *E. coli* show that lower concentrations of indole increase survival/persistence to lethal concentrations of ofloxacin, ampicillin and kanamycin (Vega et al., 2012; Vega et al., 2013), suggesting that the protective effect of indole is not specific to one family of antibiotic. Studies also pointed to the involvement of indole secretion in the cooperation between antibiotic resistant and sensitive populations during antibiotic stress (Lee et al., 2010). Notably, a recent study identified indole production as a potential target for the increased activity of quinolones against persisters in *E. coli* (Zarkan et al., 2020). Since indole appears to be beneficial for bacteria in the presence of antibiotics, we addressed whether indole production is increased upon sub-MIC AG treatment in *V. cholerae* and whether this can lead to improved response to lethal antibiotic concentrations.

Importantly, we find that indole strongly increases persistence to AGs through the action of RaiA. We find that transcription from the *raiA* gene promoter is highly upregulated in the presence of indole in exponential phase *V. cholerae* cells. RaiA was shown to be a ribosome associated protein, in the same conditions as Rmf (ribosome modulation factor) and Hpf (hibernation promoting factor) (Maki et al., 2000). The two latter factors cause dimerization of vacant 70S into inactive 100S ribosome dimers, in a process called ribosome hibernation during stationary phase (Gohara and Yap, 2018), whereas RaiA mostly binds to free 70S monosomes (Maki et al., 2000; Sabharwal et al., 2015). *E. coli* mutants lacking these ribosome-associated factors do not show any growth defect during exponential growth, which is consistent with the fact that their expression is specific to stationary phase and stress (Prossliner et al., 2018). RaiA was observed to protect the 70S ribosome from degradation (Agafonov et al., 1999; Di Pietro et al., 2013), and was also observed to block the binding of tRNA to the ribosomal A site in a cell free translation system (Agafonov et al., 2001), and during cold shock (Vila-Sanjurjo et al., 2004). In the present study, characterization of the *raiA* deletion mutant shows that RaiA is instrumental in the appearance of persister cells to AGs. We propose here a new mechanism of induced persistence to AGs by which RaiA positively affects the intact ribosome content of the cell, and facilitates regrowth after removal of the antibiotic.

Results

Indole is produced in response to sub-MIC tobramycin and increases persistence to AGs

Since the antibiotics ampicillin and kanamycin increase indole levels in *E. coli* (Han et al., 2011), we measured indole secretion (Saint-Ruf et al., 2014) in *V. cholerae* to determine whether the aminoglycoside tobramycin also impacts indole levels in this case. We found increased extracellular indole concentrations in the presence of sub-MIC tobramycin (TOB 0.15 µg/ml, 20% of the MIC, **Figure 1**). We next addressed whether indole has an impact on the growth of *V. cholerae,* using an indole concentration of 350 µM. This concentration was previously shown to be physiologically relevant in *V. cholerae* and was observed to have no inhibitory effect on growth, and to complement the biofilm formation defect of a *ΔtnaA* mutant deficient for indole production (Mueller et al., 2009). We found

that 350 µM indole does not affect growth in the absence of antibiotics, but improves growth in sub-MIC antibiotics tobramycin (**Figure S1A**).

We next addressed the effect of indole in the response to lethal concentrations of antibiotics, by measuring persister cells formation in *V. cholerae*. In order to do so, we adapted to *V. cholerae*, a protocol developed for *E. coli* (Ivan Matic and Wei-Lin Su, personal communication). Early exponential phase cultures were treated with lethal doses of antibiotics (5 to 10 times the MIC) for 20 hours. We first confirmed that cells surviving after 20 hours of antibiotic treatment and which grow upon antibiotic removal, were indeed persister cells, by performing survival curves (**Figure S2A**). The biphasic profiles of the killing curves we obtained was consistent with the formation of persister cells after 5 hours (Brauner et al., 2016). Furthermore, these cells were not resistant to the antibiotic, as no growth was observed when streaked on antibiotic containing plates (not shown). We thus carried on with the quantification of persisters at 20 hours of antibiotic treatment. We found that *V. cholerae* cultures grown in the presence of indole yielded higher numbers of persister cells to the AGs TOB and gentamicin (GEN) (**Figure 2AB**), as previously observed for *E. coli* treated with kanamycin and ofloxacin (Vega et al., 2012), but we observed no effect for persistence to carbenicillin (CRB), or trimethoprim (TMP) (**Figure 2CD**). Furthermore, a strain deleted for *tnaA* yielded less persisters to tobramycin than the WT strain (**Figure S2B**), and the effect was reversed by indole complementation, consistent with a link between indole and persistence.

Indole, at concentrations allowing growth, does not affect AG entry

We next addressed whether the beneficial effect of indole treatment in the presence of AGs is due to modifications in membrane potential, which could lead to decreased AG entry into the cell. AG uptake by the bacterial cell is known to be linked to the proton motive force (PMF). At high concentrations (5 mM) indole is a proton ionophore which blocks cell division by dissipating the PMF (Kralj et al., 2011), and was observed to interact with the cell membrane and change its physical structure (Mitchell, 2009). In order to measure AG entry in the bacterial cell, we used the aminoglycoside neomycin coupled to the fluorophore Cy-5, which was previously synthesized for aminoglycoside uptake studies in bacteria and demonstrated to bear the properties of aminoglycosides for uptake, mode of action and activity against Gram negative bacteria (Sabeti Azad et al., 2020), (Pierlé et al, unpublished). We found that indole at the physiological concentration of 350 µM does not affect AG entry into the bacterial cell (**Figure S3A**), ruling out the possibility of decreased AG entry due to modifications of PMF in the presence of indole. Moreover, the presence of 350 µM indole did not change the MIC of two aminoglycosides: tobramycin and gentamicin (**Figure S3B**). The beneficial effect of indole in the presence of AGs is thus not through reduced antibiotic entry.

Indole induces RaiA (VC0706) expression.

In order to shed light into mechanisms allowing for more efficient response to antibiotic stress upon indole treatment, we decided to study the transcriptomic changes of *V. cholerae* in response to 350 µM indole. mRNA sequencing of exponential phase cultures shows differential regulation of 260 genes shown in **Table S1** and represented in **Figure 3A** (>2-fold change, adjusted *p value* <0.01 as in (Krin et al., 2018)). The most affected categories were respiration (31 genes upregulated), electron transfer and iron uptake (55 genes downregulated). Indole mediated protection against antibiotic killing was previously proposed to be through upregulation of efflux pumps (Blair et al., 2013; Hirakawa et al., 2005; Kobayashi et al., 2006; Lee and Lee, 2010; Nikaido et al., 2012), or through an increase in OxyR associated oxidative stress response (Vega et al., 2013). However, our RNA-seq data show no induction of oxidative stress response related genes in *V. cholerae* (*oxyR*, *soxRS*, *katG*) by indole, and rather suggest decreased expression of proteins linked to iron uptake, suggesting decreased iron and ROS levels upon indole treatment (Baharoglu et al., 2013; Mehi et al., 2014). The second most affected category belongs to translation related genes (31 genes, approximately 10% of total differentially regulated genes, with *p<3.00E-4*). Notably, one translation related gene was markedly upregulated:

raiA (VC0706, 20-fold up), together with *rmf* (VC1484, 3-fold up), which are both described as factors associated with inactive ribosomes in stationary phase (Agafonov et al., 1999; Di Pietro et al., 2013). *raiA* expression is known to be triggered by transition to stationary phase (Maki et al., 2000), and RaiA is usually weakly expressed during exponential phase. RT-qPCR on *raiA* (**Figure 3B**) and fluorescence associated flow cytometry on cells carrying GFP fused to the *raiA* promoter (**Figure 4A and S4AB**) confirmed upregulation of *raiA* by indole during exponential phase, and increased expression of *raiA* in stationary phase. Since transcriptomic data pointed RaiA as one of the most differentially regulated genes by indole, we next decided to address the contribution of RaiA in the indole associated phenotypes in *V. cholerae*.

Absence of *raiA* reduces persistence to AGs and abolishes induction by indole.

In order to address the involvement of RaiA in indole induced persistence, we constructed a *V. cholerae ΔraiA* mutant, and measured the frequency of persistence to tobramycin (TOB), gentamicin (GEN), carbenicillin (CRB) and trimethoprim (TMP) in exponential phase cultures, grown in the absence and presence of indole (**Figure 2ABCD**). We found that *V. cholerae ΔraiA* generally formed slightly less persister cells to TOB, although the difference was not statistically significant when we compare persistence frequency, probably because at exponential phase *raiA* expression is not strong enough in the untreated WT strain, and due to variability between experiments. However, the ratio of persisters calculated separately for each experiment shows significant 10-fold decrease in *ΔraiA* compared to WT (**Figure S5A**). Strikingly, the deletion of *raiA* completely abolished induction of persistence by indole to both tested AGs (TOB, GEN, **Figure 2AB**), pointing to a role of RaiA in persister cell formation. No effect of neither indole nor *raiA* was observed in the formation of persisters to CRB or TMP (**Figure 2CD**), suggesting that the effect of RaiA in persister formation is specific to AGs. The involvement of RaiA in persistence to AGs also appears to be conserved in *E. coli* as the *raiA* deficient mutant yielded less persisters to TOB (**Figure S5B**). Finally, as performed above in the WT *V. cholerae* strain, we confirmed that the presence of indole does not affect the AGs MIC of the *ΔraiA* strain, and that deletion of *raiA* does not affect the MIC and AG uptake (**Figure S3AB**), meaning that the phenotypes we observe are not due to reduced entry of AGs or increased resistance. On the other hand, RaiA is dispensable for growth improvement by indole (**Figure S1B**), because indole still improves growth in TOB when *raiA* is deleted, showing that the mechanism of AG persister induction by indole (antibiotic concentration >MIC) is different than the mechanism of growth improvement in sub-MIC AGs. It is worth mentioning here that the growth of *ΔraiA* strain appeared to be slightly slower than the WT strain, suggesting that RaiA may also have a role during exponential growth, despite its low level of expression.

RaiA overexpression increases persistence to AGs and promotes earlier exit from stationary phase.

In order to mimic conditions of RaiA induction, we cloned it under a controlled P*ara* promoter, which is repressed by glucose and induced by arabinose. Since the presence of different carbon sources may differentially affect growth and the response to aminoglycosides (Pierlé et al., unpublished), and also because arabinose was shown to have an impact on growth in *V. cholerae*, we compared the persistence levels of cells carrying the empty vector (p0 in **Figure 5ABCDEF**) or the pBAD-RaiA plasmid, in the presence of arabinose (RaiA overexpression conditions). Overexpression of RaiA strongly increased persisters formation in three aminoglycosides: TOB, GEN and NEO (**Figure 5ABC**), but not in three non-aminoglycoside antibiotics from different families: CRB, TMP and ciprofloxacin (CIP) (**Figure 5DEF**), indicating that RaiA is directly and specifically involved in the persistence mechanism to aminoglycosides. Additionally, the MIC showed no difference between the *raiA* overexpression strain compared to the strain with empty plasmid p0 and pRaiA+ (MIC = 0.75 µg/ml for both on MH plates containing arabinose), ruling out a potential effect on resistance.

We next asked whether such increased persistence could be due to slower growth when RaiA is overexpressed. We monitored growth in conditions where 1) RaiA is not overexpressed previous to inoculation and only overexpressed during the growth curve, and 2) RaiA is previously overexpressed

in cells used for inoculation (**Figure S6A**). First, our results show no difference in growth rate (slope) in presence or absence of RaiA overexpression (**Figure 6AD and S6B**), indicating that RaiA overexpression does not cause a slow growth phenotype, which discards the hypothesis linking RaiA-mediated persistence to slow growth/dormancy. Interestingly, we observe in cells where RaiA overexpression was pre-induced, that these cells start growing faster due to a reduction in lag phase (**Figure 6BC and Figure S6B**). Such a reduction in lag phase is reminiscent of increased active ribosome content which allows faster resumption of growth at the exit of stationary phase (Condon et al., 1995). As a corollary, when *raiA* was deleted, the lag phase was increased (**Figure 7A and Figure S6C**), suggesting that RaiA levels affect inactive but "ready to use" ribosome content, which we called *sleeping ribosomes*, in stationary phase.

The effect of RaiA on lag phase and persistence is independent of ribosome hibernation factors Rmf/Hpf

RaiA was previously found to be associated with the inactive ribosomes at stationary phase, in the same conditions as Rmf and Hpf factors. Rmf and Hpf are known to dimerize ribosomes into so called hibernating 100S ribosomes, whereas RaiA associates with monomeric 70S ribosomes (Gohara and Yap, 2018; Maki et al., 2000; Prossliner et al., 2018). In order to address whether Hpf/Rmf dependent ribosome hibernation also favors rapid exit from stationary phase, we performed deletion and overexpression experiments similar to what we did for RaiA. Deletion of *rmf* or *hpf* has no effect on lag phase nor growth (**Figure 7A and S6C**). Our results showed that in contrast to overexpression of RaiA which decreases the lag phase, overexpression of Rmf or Hpf rather increase lag phase (F**igure 7B and S6C**). These findings are consistent with a model where increased ribosome dimerization by Hpf/Rmf would require action of dissociation factors in order to resume growth whereas spontaneous dissociation of RaiA from inactive 70S ribosomes (Agafonov et al., 2001; Maki et al., 2000), is sufficient for growth restart. Furthermore, when we overexpressed RaiA in Δ*hpf* or Δ*rmf* mutants, we observed a reduction of lag phase similar to what is observed upon overexpression of RaiA in the WT strain (**Figure 7DC**), meaning that RaiA action is not dependent of Hpf/Rmf mediated ribosome hibernation.

In addition, we addressed the effect of hibernation factors on persistence in exponential phase. Unlike for RaiA overexpression, no increase in persistence to TOB was detected upon overexpression of Hpf or Rmf, excluding an effect of 100S ribosome dimer formation on persistence to AGs in exponential phase (**Figure 5A**). Unexpectedly, persistence levels even decreased upon overexpression of Hpf, suggesting that 70S-RaiA (sleeping ribosome) and 100S-Rmf/Hpf (hibernating ribosome) complexes may have opposite effects on persistence to AGs in exponentially growing bacteria. We also tested the persistence levels of *rmf* and *hpf* deletion mutants. Surprisingly again, and consistent with overexpression results, we found that deletion of *rmf* or *hpf* hibernation factors increases persistence to AGs (**Figure S7**). The increase of persistence due to deletion of *rmf* is dependent on the presence of *raiA*, as the double mutant *raiA rmf* shows reduced persistence compared to WT, and similar to the *raiA* mutant. This can be due to the observed increased expression of *raiA* in the absence of *rmf* (Sabharwal et al., 2015) or amplified ribosome-RaiA complex formation in the absence of *rmf,* due to decreased 100S formation (Ueta et al., 2005). Finally, it is important to note that the *hpf raiA* double mutant could not be constructed despite the use of two different strategies, implying synthetic lethality. Overall these results suggest an equilibrium between Rmf/Hpf and RaiA actions, consistent with previous literature that showed a combined role for these proteins in ribosome hibernation and antagonizing regulation of *rmf/hpf* and RaiA in *V. cholerae* (Sabharwal et al., 2015).

RaiA overexpression increases 70S ribosome proportion over 50S and 30S subunits in stationary phase.

In order to address whether intact 70S ribosomes are protected/stored upon RaiA overexpression, we measured the ribosome contents of WT and RaiA overexpressing cells, as well as the strain deleted for

raiA, by performing 10-50% sucrose gradients on cellular extracts from 24h stationary phase cultures. The profiles obtained were consistent with well described peaks for 30S and 50S subunits followed by a third peak corresponding to the 70S ribosome (Ueta et al., 2013). No clear 100S peak was observed in any of the experiments. Deletion of *raiA* leads to a slight increase in the proportion of dissociated subunits compared to 70S ribosome. We found that the proportion of 70S ribosomes is increased compared to 30S+50S dissociated subunits upon RaiA overexpression (**Figure 8AB**). This agrees with the hypothesis that RaiA would stabilize the intact 70S ribosome and increase functional ribosome pools, reducing the lag phase of the population upon growth restart.

RaiA expression is under environmental control and linked to the Fur iron sensing regulon in *V. cholerae*

RaiA is known to be expressed in stationary phase and upon temperature stress (Agafonov et al., 1999; Agafonov et al., 2001; Maki et al., 2000; Sabharwal et al., 2015; Slamti et al., 2007). Regulation of *raiA* was also described to occur through carbon catabolite control (CRP-cAMP) (Manneh-Roussel et al., 2018; Shimada et al., 2013). Our transcriptomic data suggests that indole affects genes from the Fur regulon (**Table S1**). Fur responds to iron levels and is generally known to be a repressor of iron/heme transport genes (such as *hutA*, *hutXW*, *tonB*, *fbpA*, *viuB*, among others) and also activates a small number of genes (namely the *napABC* operon and *menB* in *V. cholerae*) (Mey et al., 2005). The *V. cholerae raiA* gene promoter, appears to carry sequences similar to Fur boxes described in *V. cholerae* (Davies et al., 2011). In order to shed light in the means by which indole induces expression from the *raiA* promoter in exponential phase, we constructed deletion mutants for *fur*, *crp* and for the stationary phase sigma factor *rpoS.* We used our *PraiA-gfp* transcriptional fusion to measure expression in the presence and absence of indole in the mutants compared to wild type strain.

As expected, in WT *V. cholerae*, fluorescence was triggered by indole at 3 hours of culture which corresponds to early exponential phase (OD 0.2 to 0.3), and accumulated in stationary phase (**Figure 4A and S4AB**). Deletion of *crp* strongly decreases *raiA* expression (25x in exponential phase, **Figure 4B and S4AB**), confirming that CRP is a prevailing activator of *V. cholerae raiA*. On the other hand, deletion of *rpoS* had no major effect on *V. cholerae raiA* expression (1.25x decrease). In the *Δfur* strain, *raiA* expression was increased 2-fold (**Figure 3B and S4AB**), suggesting Fur dependent repression of the *raiA* promoter. No major effect on *raiA* promoter was observed upon treatment with iron, possibly because iron is already in excess levels for the cells during growth. Strikingly, treatment with dipyridyl (DP), an iron chelator which mimics conditions of iron starvation strongly induced fluorescence (**Figure 4A**). To confirm that these effects were specific to the *raiA* promoter, we introduced constitutively expressed *gfp* using the same plasmid vector in the strains WT, *Δcrp* and *Δfur* and observed no effect on fluorescence (**Figure S8**). This was also the case upon indole treatment of the WT strain. DP appears to decrease fluorescence for constitutive promoter, while increasing it 4x from *raiA* promoter (**Figure 3B**). Overall, these data confirm that decreased fluorescence in *Δcrp* and increased fluorescence in *Δfur* or upon indole and DP treatments are specific to an effect on transcription from the *raiA* promoter.

These results show a link between extracellular iron levels and RaiA expression. Together with the CRP-cAMP control, RaiA expression appears to be under environmental control, highlighting a link between bacterial persistence and environmental stress.

The effect of RaiA overexpression is conserved in the Gram-negative pathogen *Pseudomonas aeruginosa*.

We next asked whether RaiA could have a similar function in other Gram-negative pathogens such as *Pseudomonas aeruginosa*, an organism associated with antibiotic resistance and persistence (Koeva et al., 2017; Spoering and Lewis, 2001) and of high concern regarding resistant infections. *P. aeruginosa* RaiA exhibits 37% protein identity with RaiA from *V. cholerae*. We overexpressed *V. cholerae* RaiA in *P. aeruginosa* and assessed lag phase and persistence, as we performed for *V. cholerae.* We found that

upon RaiA overexpression, lag phase is also decreased in *P. aeruginosa* (**Figure 9A and S6D**), and strikingly, persistence to tobramycin is increased (**Figure 9B**). These results show that RaiA-protected sleeping ribosomes can be involved in persistent infections by various pathogenic bacteria.

Discussion

We show here that indole is produced upon sub-MIC aminoglycoside treatment in *V. cholerae* and at physiological concentrations, and increases appearance of persister cells in lethal concentrations of AGs. We find that such increase in persistence occurs through an inducible mechanism involving RaiA (previously called pY or *yfiA* in *E. coli*, and *vrp* in *V. cholerae*). While indole improved growth in the presence of sub-MIC antibiotics seems to be nonspecific to an antibiotic class and independent of RaiA, increased persistence involving RaiA is specific to AGs in exponentially growing bacteria. Since RaiA is regulated by several environmental cues and signaling molecules, our findings highlight a new, inducible mechanism of persistence, based on increased protection of ribosomes during stress, rather than slowdown of the metabolism.

In vitro characterization of RaiA in *E. coli*, has previously shown association with ribosomes during cold shock and stationary phase, but not during growth at 37°C, suggesting that binding of RaiA is prompted by stress (Agafonov et al., 2001). Based on crystal structures, RaiA was suggested to arrest translation (Vila-Sanjurjo et al., 2004). However, our results in *V. cholerae* do not support such a role, since there is no impact of RaiA overexpression on growth, and rather point to a protective effect of RaiA under ribosomal stress caused by AG treatment.

Alternatively, since RaiA is able to stabilize the 70S ribosome monomers against dissociation *in vitro* (Agafonov et al., 1999; Di Pietro et al., 2013), it was proposed to constitute a pool of inactive 70S ribosomes preserved from degradation in bacteria (Giuliodori, 2016; Giuliodori et al., 2007; Gualerzi et al., 2011).

In vivo effects of RaiA on bacterial phenotypes are less well described. A protective effect of RaiA during stress, such as starvation, was previously observed in the Gram-positive species *Mycobacterium tuberculosis* (Li et al., 2018) and *Lactococcus lactis* (Puri et al., 2014). Yet, the mechanisms remained enigmatic. Our results show a role of RaiA on survival to antibiotic stress in Gram-negative pathogens.

One known mechanism of protection of non-translating ribosomes is ribosome hibernation. The ribosome hibernation factors, Rmf (ribosome modulation factor) and Hpf (hibernation promoting factor) (Maki et al., 2000), dimerize 70S ribosomes (monosomes) into 100S hibernating ribosome dimers. The importance of ribosome hibernation in stress survival is well established in various bacteria (McKay and Portnoy, 2015; Tkachenko et al., 2017), as 100S dimers are less susceptible to degradation by RNases (Feaga et al., 2020; Prossliner et al., 2018; Prossliner et al., 2021; Wada et al., 2000; Yamagishi et al., 1993). Ribosome hibernation factors were even proposed as potential new targets for antibiotics (Matzov et al., 2019). However, in some cases, 70S particles appear to be more robust during heating than 100S dimers which dissociate into 30S and 50S subunits more rapidly (Niven, 2004).

RaiA was previously identified as bound to the ribosome together with Rmf and Hpf, but its role in relation with ribosome hibernation is unclear. In *V. cholerae*, RaiA shows a synergistic effect with Hpf for survival to starvation (Sabharwal et al., 2015), and we observe a synthetic lethal phenotype for the deletion of *raiA* and *hpf*. Despite such apparent synergy with hibernation factors, RaiA was shown to inactivate 70S ribosomes without forming 100S dimers (Polikanov et al., 2012; Ueta et al., 2005). RaiA thus appears to act in a process different than ribosome hibernation, maybe by blocking breaking down of ribosomes into 30S and 50S subunits by ribosome recycling factors (Rrf/EF-G) (Agafonov et al., 1999; Janosi et al., 1996).

In *E. coli*, RaiA can even prevent 100S dimer formation by Hpf and Rmf (Maki et al., 2000; Ueta et al., 2005). According to cryo-EM data, RaiA can compete with Rmf for ribosome binding, hence shifting the ribosome content from a Rmf-mediated dimeric inactive form to a RaiA-bound monomeric inactive form (Franken et al., 2017). Recent work has identified RaiA as a player in persister formation together with hibernation factors, through a dormancy related mechanism linked to stringent response/ppGpp

(Song and Wood, 2020; Wood and Song, 2020). In these studies, persister formation was assessed on near stationary cell cultures (OD 0.8), where these factors are highly expressed, and persistence is largely due to dimerization of inactive ribosomes, leading to a general dormancy state which also favors persister formation to other antibiotics like ampicillin and ciprofloxacin. In contrast, the present study shows in exponentially growing cells and without nutrient limitation, a specific mechanism involving the induction of RaiA, triggering persistence specifically to aminoglycosides (and not to other antibiotics), without affecting growth (**Figure 10A**). The mechanism we describe is also different than the ppGpp-independent persistence caused in slow growing bacteria (Pontes and Groisman, 2019), since increased RaiA does not affect growth rate in our study. In this regard, the RaiA-dependent persistence mechanism observed in the present study is not a dormancy-like or slow growth mechanism, unlike the increased persistence triggered by ppGpp to antibiotics from various families, in stationary phase. Moreover, no effect of hibernation factors Rmf/Hpf is observed, suggesting different persistence mechanisms than ribosome dormancy formation in growing cells. Recent studies also show the existence of mechanisms triggering persistence independently of ppGpp or hibernation factors in bacteria (Hossain et al., 2021; Wood et al., 2021). We show here that RaiA is one player enhancing persister formation in the Gram-negative bacterium *V. cholerae.*

While RaiA, Hpf and Rmf are rapidly released from ribosomes when normal growth conditions are restored (Agafonov et al., 2001; Maki et al., 2000), ribosome reactivation necessitates dissociation of hibernating 100S ribosome dimers into monomers by HflX and other factors (Basu and Yap, 2017), whereas no dissociation factor is needed for the reactivation of the RaiA inactivated 70S ribosome. There may thus be an interplay and equilibrium between hibernating 100S-Hpf/Rmf and "sleeping" 70S-RaiA forms.

Such synergy or antagonism between inactive 70S and 100S ribosome pools can however depend on the nature of the stress and the bacterial species. We show here that persistence to aminoglycosides is better achieved in the presence of RaiA (70S), rather than hibernation factors (100S) in *V. cholerae*. Here, we propose that increased production of RaiA (e.g. upon stress) leads to preservation of non-translating ribosomes in a pool of inactive and intact 70S "sleeping" ribosomes. In that scenario, bacteria can keep growing in the absence of the antibiotic, since RaiA will not bind to actively translating ribosomes. Upon stress affecting translation (e.g. aminoglycosides), ribosomes may stall or stop, which would lead to the dissociation from the mRNA. If RaiA is induced, we propose that such non-translating 70S ribosomes will be bound and protected by RaiA, and avoid death upon antibiotic treatment, not by entering a dormant state, but by inducing protection of ribosomes**.** We propose that, in contrast to hibernating ribosomes which need recycling factors to dissociate into 70S monosomes, such sleeping ribosomes can be rapidly reactivated upon stress relief through spontaneous dissociation of RaiA from the intact 70S monosome (Agafonov et al., 2001; Maki et al., 2000), conferring an advantage for stress survival (**Figure 10AB**).

In line with this, a recent study showed that the greater the ribosome content of the cell, the faster persister cells resuscitate (Kim et al., 2018). In parallel, protein synthesis was shown to be necessary for persister cell formation in *V. cholerae* (Paranjape and Shashidhar, 2019), consistent with the fact that we see no effect of RaiA overexpression on growth rates, thus on protein synthesis during growth. Our results do not exclude however another role for RaiA on translating ribosomes.

Increased RaiA levels thus allow higher persistence, but what is controlling RaiA expression? RaiA is expressed in stationary phase and during cold shock (Agafonov et al., 1999; Agafonov et al., 2001; Maki et al., 2000; Sabharwal et al., 2015). Other known factors are the heat shock in *V. cholerae* (Slamti et al., 2007), stringent response (Prossliner et al., 2018), envelope stress and the carbon catabolite response (Manneh-Roussel et al., 2018; Shimada et al., 2013). We additionally show that *raiA* expression is linked to iron levels and responds to Fur regulation. Interestingly, iron associates with ribosomes (Bray et al., 2018) and a link between iron and modulation of ribosome function during stress has been described (Zinskie et al., 2018). Iron control of RaiA may thus allow protection of

ribosomes from iron related damage. Altogether, RaiA appears to be part of the bacterial response to environmental stress.

Results of the present study constitute a link between bacterial signaling, ribosome protection and persistence. Moreover, since RaiA action appears to be conserved in various pathogens (Gram-negatives and positives, such as *S. aureus* and *M. tuberculosis*), it may be one factor involved in the failure of treatment in persistent infections. It would be interesting to ask now whether RaiA can be used as an early indicator of persistence, which would allow isolation of persisters within a heterogeneous population and further studies using single cell approaches.

Limitation of Study

This study shows that indole is secreted under sub-MIC aminoglycosides treatment and increases *raiA* expression. It also shows that indole is implicated in *raiA*-dependent persister formation under lethal aminoglycosides treatment. However, we do not address whether indole is also produced under lethal treatment because it is challenging to quantify indole production or *tnaA* expression on dying cells. Development of this method in our lab could be the purpose of a future work.

In addition, *raiA*-dependent persister formation is shown here to be specific to aminoglycosides (bactericidal), which target translation. Bacteriostatic antibiotics such as chloramphenicol or tetracycline also target the ribosome, but persistence assays are usually not performed using these antibiotics. Our study does not exclude a role for *raiA* protection on sleeping in the response to such translation targeting antibiotics.

Author Contributions

Experiments were designed by Z.B. Experiments were conducted by M.L., E. K., C.K. and Z. B., and results were interpreted by Z.B. and M.L. RNA-seq library preparation, sequencing and statistical analysis was performed by O. S., H.V. and J-Y. C. The manuscript was written and reviewed by Z.B., M.L. and D.M. All authors read and approved the final manuscript.

Declaration of Interests

The authors declare no competing interests.

Acknowledgements

We are thankful to Micheline Fromont-Racine for her valuable help with the experiments for ribosome content analysis by sucrose density gradients. We thank Ivan Matic, Wei-Lin Su and Sébastien Fleurier for helpful discussions and Ivan Matic for critical reading of the manuscript. We also thank Sebastian Aguilar Pierlé for advice for Neo-Cy5 uptake experiments. We thank Louna Fruchard for help with persistence assays. This work was supported by the Institut Pasteur, the Centre National de la Recherche Scientifique (CNRS-UMR 3525), the Fondation pour la Recherche Médicale (FRM Grant No. DBF20160635736), ANR Unibac (ANR-17-CE13-0010-01) and Institut Pasteur grant PTR 245-19.

Main Figure Titles and Legends

Figure 1. Indole is produced during growth in sub-MIC tobramycin and induces *raiA*. Measure of extracellular indole concentrations of bacterial cultures grown overnight in rich medium MOPS (Teknova EZ rich defined medium) with and without tobramycin at 0.10 µg/ml (TOB 0.10) or 0.15 µg/ml (TOB 0.15) using the Kovacs reagent (Saint-Ruf et al., 2014). *ΔtnaA* strain was used as negative control without tobramycin. Experiments were performed in triplicates, and statistical analysis was performed (***: *p<0.001*). Error bars represent standard deviation.

Figure 2. Modulation of persistence of exponential phase WT and *ΔraiA V. cholerae* by indole. A to D: Early exponential phase of wild-type (WT) and *ΔraiA V. cholerae* cultures were treated with lethal doses of the specified antibiotics for 20 hours. The y axis represents survival, as the number of CFU

growing after antibiotic treatment and removal divided by the total number of CFU at time zero (before antibiotic treatment). Bars represent geometric means and error bars represent geometric standard deviation. Tobramycin (TOB): 10 µg/ml, gentamicin (GEN): 5 µg/ml, carbenicillin (CRB): 100 µg/ml, indole (IND): 350 µM. Experiments were performed 3 to 6 times, and statistical analysis was performed (*: *p <0.05;* **: *p<0.01*).

Figure 3. **Indole production during growth in sub-MIC tobramycin induces *raiA*. A.** Volcano plot showing differentially expressed genes upon indole treatment. X axis represents log 2-fold change, Y axis represents the negative log 10 of the *p value*. *raiA*, *rmf* and *hpf* are indicated. The dashed line represents a *p value* of 0.01, all of the dots above thus show a *p value*<0.01. Red dots indicate genes linked with respiration, green with sugar metabolism, dark blue with iron, purple with amino-acid metabolism, and light blue with translation. RNA-seq was performed in triplicates for each condition. See also Table S1. **B.** *raiA* mRNA levels measured by RT-qPCR on exponential phase *V. cholerae* cultures in presence or absence of indole. Statistical analysis was performed (**: *p<0.01*). Error bars represent standard deviation.

Figure 4. Environmental stress induce *raiA* expression in exponential phase *V. cholerae*. Fluorescence quantification of GFP expression from the *raiA* promoter by flow cytometry in MH media in exponential phase (except for "Stat"). **A. in WT *V. cholerae***. NT: Non-treated, IND: indole (350 µM), Fe: iron (18 µM), DP: 2,2'-Dipyridyl (500 µM), Glc: Glucose (1%), Mal: Maltose (1%), Stat: stationary phase. The y axis represents the fluorescence ratio of the treated over non-treated (NT) strain. **B. in indicated *V. cholerae* deletion mutants**. The y axis represents the fluorescence ratio of the mutant over wild type (WT) strain. Mean fold change values are indicated within histogram bars. Experiments were performed at least 3 times, and statistical analysis was performed (**: *p <0.01;* ****: *p<0.0001*). Error bars represent standard deviation. See also **Figure S4.**

Figure 5. **Modulation of persistence of exponential phase *V. cholerae* by RaiA.** Early exponential phase of wild-type (WT) *V. cholerae* carrying either the empty pBAD vector (p0) or with specified gene (pGene) cultures were treated with lethal doses of the specified antibiotics for 20 hours. The y axis represents survival, as the number of CFU growing after antibiotic treatment and removal divided by the total number of CFU at time zero (before antibiotic treatment). Tobramycin (TOB): 10 µg/ml, gentamicin (GEN): 5 µg/ml, carbenicillin (CRB): 100 µg/ml, ciprofloxacin (CIP): 0.025 µg/ml, trimethoprim (TMP): 50 µg/ml, neomycin (NEO): 30 µg/ml, indole (IND): 350 µM. Experiments were performed 3 to 6 times, and statistical analysis was performed (*: *p <0.05;* **: *p<0.01*).

Figure 6. RaiA influences lag phase upon growth restart after the stationary phase. Growth is measured on a TECAN plate reader. The curves of wild type *V. cholerae* with the empty plasmid are compared with plasmid carrying *raiA* under inducible promoter in MH media containing either glucose or arabinose. The promoter is repressed using glucose (GLC) and induced using arabinose (ARA). Growth was performed as specified, with RaiA expression repressed or induced in the overnight culture used for inoculum (overnight culture supplemented or not with ARA; indicated as "*during pre-cultures"*), or/and with RaiA expression induced or not during growth in the microplate reader (growth media supplemented or not with ARA in the microplate; indicated as "*during sub-cultures"*) : **A.** GLC/ARA, **B**. ARA/GLC, **C.** ARA/ARA, **D.** GLC/GLC**.** A scheme of the experimental setup is found on Figure S5A. Experiments were performed in triplicates and geometric means are represented. Error bars represent the geometric standard deviation. See also **Figure S6B**.

Figure 7. The effect of RaiA on lag phase is independent of ribosome hibernation factors Rmf/Hpf. A. Growth in MH media of WT and mutant strains. **B**. Growth of *V. cholerae* overexpressing hibernation

factors or empty plasmid in MH media containing arabinose (ARA/ARA). **CD**: Growth of hibernation factor mutants Δ*rmf* and Δ*hpf* overexpressing RaiA in MH media containing arabinose (ARA/ARA). Experiments were performed in triplicates and geometric means are represented. Error bars represent the geometric standard deviation. See also **Figure S6C**.

Figure 8. RaiA levels influence stationary phase 70S ribosome content relative to 50S+30S subunits in *V. cholerae*. A. Cellular extracts of 24 hours cultures (Δ*raiA* and WT *V. cholerae* carrying the p0/pBAD-RaiA vector, in MH media containing spectinomycin and arabinose) were separated on 10-50% sucrose density gradient. Ribosomal RNA content was measured at OD 260 nm using a spectrometer coupled to a pump and time on X axis represents samples from less dense (upper fragments, smaller complexes) to denser (bottom of the tube, heavier complexes). Lysis was performed in the presence of 10 mM $MgCl_2$. Cell debris eluting before 550 seconds are not shown. Graphs are normalized to total OD 260 nm =1 for each sample. Mean values are indicated within histogram bars. Error bars represent standard deviation. **B.** Percentage of 70S ribosomes over total ribosome subunits (70S)/(70S+50S+30S). Error bars represent standard deviation (**: $p<0.01$).

Figure 9. RaiA overexpression in *Pseudomonas aeruginosa* increases tolerance to tobramycin in exponential phase and promotes earlier exit from stationary phase. A. Growth is measured on a TECAN plate reader. The curves of WT *P. aeruginosa* with the empty plasmid (p0) are compared with the plasmid carrying *raiA* of *V. cholerae* under inducible promoter in MH media containing arabinose**.** See also **Figure S6D B**. Early exponential phase of WT *P. aeruginosa* cultures were treated with lethal doses of tobramycin (TOB: 10 µg/ml) for 20 hours. The y axis represents survival, as the number of CFU growing after antibiotic treatment and removal divided by the total number of CFU at time zero (before antibiotic treatment) (*: $p<0.05$). Experiments were performed in triplicates.

Figure 10. **Summary model: RaiA mediated ribosome protections increases persistence to aminoglycosides and decreases lag phase during growth restart**. Diagrams depict RaiA induced conditions. **A. Persistence**. During exponential growth, treatment with lethal doses of aminoglycosides leads to disruption of translation and stalling of translating 70S ribosomes, and eventually to their dissociation into 50S+30S subunits and degradation of these ribosomes, resulting in cell death. Upon induction of RaiA (e.g. by indole signaling), we propose that RaiA does not affect translating ribosomes, but binds non-translating 70S ribosomes to form sleeping ribosomes, and protects them from dissociation into subunits and degradation. This results in increased persistence. **B. Length of lag phase**. In a stationary phase culture (e.g. overnight culture), translation is highly decreased, leading to dissociation from the mRNA ribosome degradation. Upon growth restart, a lag phase thus occurs where ribosomes are resynthesized. We propose that when RaiA production is increased before entering the stationary phase, an increased proportion of non-translating ribosomes are bound and are preserved as 70S by RaiA, rather than being degraded. The presence of such an increased pool of intact 70S ready-to-use sleeping ribosomes gives an advantage on translation reactivation, while degraded ribosome have to be recycled or de novo synthetized, decreasing the lag phase necessary for the synthesis of a sufficient number of ribosomes.

STAR METHODS

RESOURCE AVAILABILITY

Lead contacts

Further informations and requests for resources and reagents should be directed to and will be fulfilled by the Lead Contacts, Didier Mazel (didier.mazel@pasteur.fr) or Zeynep Baharoglu (baharogl@pasteur.fr).

Materials availability

This study did not generate new unique reagents.

Data and code availability

RNA-seq data are deposited at GEO: GSE182561

EXPERIMENTAL MODEL AND SUBJECT DETAILS

Bacterial Strains and Plasmids

All *V. cholerae* strains used in this study are derivative of *V. cholerae* N16961 *hapR*+, and were constructed by allelic exchange. All *E. coli* strains used in this work are derivatives of *E. coli* MG1655, and were constructed by transduction using *E. coli* Keio knockouts strains. Strains and plasmids are listed in Key Resources Table, and Table S2 for more details.

Media and Growth Conditions

Vibrio cholerae: Colonies on plates grew at 37°C, in MH media. Plates are conserved at room temperature and should not be placed at 4°C. Liquid cultures grew at 37°C in appropriate media (see Methods), in aerobic conditions, with 180 rotations per minute. *E. coli* and *P. aeruginosa*: Colonies on plates grew at 37°C, in MH media, and are conserved at 4°C. Liquid cultures grew 37°C in aerobic condition in appropriate media (see Methods), with 180 rotations per minute.

METHOD DETAILS

Persistence tests. Persistence tests were performed on early exponential phase cultures. In order to clear the culture from previously non-growing cells that could potentially be present from the stationary phase inoculum, we performed a two-step dilution protocol, before antibiotic treatment. For overexpression experiments, glucose 1% was added to the overnight cultures to repress the pBAD promoter. Overnight *V. cholerae* cultures were first diluted 1000x in 4 ml fresh Mueller-Hinton (MH) medium, without indole (with the antibiotic allowing to maintain the plasmid and incubated at 37°C with shaking. For overexpression experiments, arabinose 0.2% was added at this first dilution step to the fresh MH media to induce the pBAD promoter. When the OD 620 nm reached ~0.2, cultures were diluted 1000x a second time, in order to clear them from non-growing cells, in Erlenmeyers containing 25 ml fresh MH medium, without or with indole at 350 µM (with the antibiotic allowing to maintain the plasmid, when the strain carried a plasmid), and were allowed to grow at 37°C. For overexpression experiments, arabinose 0.2% was added again at this second dilution step to the fresh MH media to induce the pBAD promoter. When cultures reached an OD 620 nm between 0.25 and 0.3 (early exponential phase), appropriate dilutions were plated on MH plates to determine the total number of CFUs in time zero untreated cultures. Note that for *V. cholerae*, it was important to treat cultures at the precise OD 620 nm 0.25-0.3, as persistence levels seem to be particularly sensitive to growth phase in this species, where they decline in stationary phase, and because we wanted to avoid any stationary phase protein expression such as *raiA* or *rpoS* at later growth. 5 ml of cultures were collected into 50 ml Falcon tubes and treated with lethal doses of desired antibiotics (5-10 times the MIC: tobramycin 10 µg/ml, gentamicin 5 µg/ml, neomycin 30 µg/ml, carbenicillin 100 µg/ml, ciprofloxacin 0.025 µg/ml, trimethoprim 50 µg/ml) for 20 hours at 37°C with shaking in order to guarantee oxygenation. The same

protocol was used for persistence assays on *P. aeruginosa*. Appropriate dilutions were then plated on MH agar without antibiotics and proportion of growing CFUs were calculated by doing a ratio with total CFUs at time zero. Experiments were performed 3 to 6 times.

Quantification of extracellular indole concentrations. Extracellular indole concentration was measured on bacterial cultures grown overnight with and without antibiotics using the Kovacs reagent (Saint-Ruf et al., 2014). First, we established an indole concentration standard curve using 1 ml culture medium (without bacteria) supplemented with indole 0 to 1000 µM (100 µM steps). After adding 500 µl KOVACS reagent, 100 µl of the top layer of the reaction was mixed with 800 µl isoamyl-HCl and OD was read at 570 nm. For indole measurement on bacterial samples, 1 ml of culture was subjected at the same protocol. Measured indole concentration was normalized to the bacterial dry mass based on the assumption that for an OD 600 nm = 1 bacterial dry mass is 0.3 mg/ml (Soini et al., 2008). We detected no indole production in MH medium in any condition. In order to quantify secreted indole in the presence and absence of sub-MIC antibiotics, we thus used the defined rich MOPS transparent medium (Teknova EZ rich defined medium), where MIC TOB is 0.75 µg/ml. All the following experiments (persistence, growth) were conducted in MH, as it allows to study the impact of defined indole concentrations added to the media.

Quantification of fluorescent neomycin uptake was performed as described (Pierlé et al, manuscript in revision, (Okuda, 2015; Sabeti Azad et al., 2020)). Neo-cy5 is an aminoglycoside coupled to the fluorophore Cy5, and has been shown to be active against Gram- bacteria (Okuda, 2015; Sabeti Azad et al., 2020). Briefly, overnight cultures were diluted 100-fold in rich MOPS (Teknova EZ rich defined medium). When the bacterial strains reached an OD 620 nm of 0.25, they were incubated with 0.4 µM of Cy5 labeled Neomycin for 15 minutes at 37°C. 10 µl of the incubated culture were then used for flow cytometry, diluting them in 250 µl of PBS before reading fluorescence. WT *V. cholerae*, was incubated simultaneously without Neo-Cy5 as a negative control. Flow cytometry experiments were performed as described (Baharoglu et al., 2010) and repeated at least 3 times. For each experiment, 100,000 events were counted on the Miltenyi MACSquant device.

MIC determination using etests. Stationary phase cultures were diluted 20 times in PBS, and 300 µL were plated on MH plates and dried for 10 minutes. etests (Biomérieux) were placed on the plates and incubated overnight at 37°C.

RNA-seq. Overnight cultures of the O1 biovar El Tor N16961 *hapR+ V. cholerae* strain were diluted 100x and grown in triplicate in MH medium until an OD 620 nm = ~0.4 with or without 350 µM indole. Sample collection, total RNA extraction, library preparation, sequencing and analysis were performed as previously described (Krin et al., 2018).

***raiA* qRT-PCR.** Total RNA was extracted and purified from exponential phase cultures in MH in presence or absence of indole, as previously described (Krin et al., 2018). Reverse transcription (RT) was performed on 100 ng total RNA using SuperScript® III First-Strand Synthesis System for RT-PCR (Invitrogen). Quantitative PCR was performed on 2 µl RT sample diluted 10-fold using SYBR Green PCR Master Mix (APPLIED) and QuantStudio 6. Quantification was performed using standard range. Expression values were normalized against *gyrA* as previously described in *V. cholerae* (Liu et al., 2010; Lo Scrudato and Blokesch, 2012).

Quantification of raiA expression by fluorescent flow cytometry using a gfp fusion. gfp was amplified by PCR using primers carrying the raiA promoter region and cloned into pTOPO-TA cloning vector. The PraiA-gfp fragment was then extracted using EcoRI and cloned into the low copy plasmid pSC101 (1 to 5 copies per cell). The plasmid was introduced into desired strains, and fluorescence was measured on

indicated conditions, by counting 100,000 cells on the Miltenyi MACSquant device. Likewise, the control plasmid Pc-gfp (constitutive) was constructed using primers ZIP513/ZIP200 and similarly cloned in pSC101.

Growth curves. Overnight cultures were diluted 100x in fresh medium, on 96 well plates. Each well contained 200 µl. For overexpression lag experiments, glucose 1% was added to the media to repress the pBAD promoter while arabinose 0.2% was added to the media to induce the pBAD promoter, and same growth conditions (glucose or arabinose) were compared in order to avoid noise due to the effects of arabinose on growth and cells shape in *V. cholerae* (Espinosa et al., 2020). Spectinomycin was also added during each experiment to maintain the plasmid. Plates were incubated with shaking on TECAN plate reader device at 37°C, OD 620 nm was measured every 15 minutes.

Preparation of cell lysate for the analysis of ribosome content. The protocol was adapted from (Qin and Fredrick, 2013). Since we used stationary phase cultures instead of exponential phase, presence of polysomes is not expected. 10 ml of 20 hours cultures were centrifuged in ice cold 50 ml Falcon tubes for 15 minutes at 5000 rpm at 4°C. Pellets were resuspended in 500 µl lysis buffer (10 mM Tris-HCl, pH 8, 10 mM $MgCl_2$, Lysozyme 1 mg/ml, protease inhibitor), transferred in ice cold 1.5 ml tubes and incubated with 12 µl Ribolock RNase inhibitor (Thermo scientific) and DNaseI (5 U/ml) at 4°C for 15 minutes. Cell lysis was performed through 3 cycles of flash-freezing in dry ice and thawing in a water bath at 4°C. 15 µl of 10% sodium deoxycholate were added and cell lysate was obtained after centrifugation at 10,000 rpm for 10 minutes at 4°C. The pellet containing cell debris was discarded. Lysate was kept at -80°C until sucrose gradient ultracentrifugation.

Sucrose gradient. 10-50% sucrose gradient tubes (Beckman ULTRA CLEAR) were prepared. 2U of OD 260 nm of each cell extracts were deposited on sucrose gradient tubes. Ultracentrifugation was performed at 39,000 rpm at 4°C for 2 hours 45 minutes. Fractions were collected using a pump coupled to a spectrometer at OD 260 nm, and plotted as a function of time (seconds).

Quantification and statistical analysis. First an F-test was performed in order to determine whether variances are equal or different between comparisons. For comparisons with equal variance, Student's t-test was used. For comparisons with significantly different variances, we used Welch's t-test. For multiple comparisons, we used one-way ANOVA. We used GraphPad Prism to determine the statistical differences between groups. **** means $p<0.0001$, *** means $p<0.001$, ** means $p<0.01$, * means $p<0.05$. Number of replicates for each experiment was $3<n<6$. Means and geometric means for logarithmic values were also calculated using GraphPad Prism. For persistence tests, data were first log transformed in order to achieve normal distribution, and statistical tests were performed on these log-transformed data.

Supplemental Data

Table S1. Differentially expressed genes upon indole treatment. Related to Figure 3.

Table S2. Strains and plasmids. Related to STAR Methods.

Supplementary figures legends.

Figure S1. Indole improves growth of *V. cholerae* in the presence of tobramycin. A. WT**. B.** Δ*raiA*. Growth is measured on a TECAN plate reader. IND: indole 350 µM. TOB: tobramycin sub-MIC (0.6 µg/ml). Experiments were performed in triplicates and geometric means are represented. Error bars represent the geometric standard deviation. Related to **Figure 1**.

Figure S2. Persistence and the effect of indole. A. Kinetics of survival of WT *V. cholerae* to tobramycin 10 µg/ml in MH media. Time zero corresponds to the total number of CFU before addition of antibiotics, to an early exponential phase culture (OD 620 nm 0.25-0.3), as described in the methods section. The proportion of surviving cells is calculated after plating and counting growing colonies, and is represented for each time point. Curves represent geometric means of at least 3 replicates for each time point and error bars represent geometric standard deviation. **B**. Persistence of *V. cholerae* WT and Δ*tnaA* mutants in exponential phase (in LB instead of MH, to allow indole production, see methods) after 20 hours treatment with specified antibiotics. Tobramycin (TOB): 10 µg/ml, carbenicillin (CRB): 100 µg/ml. Related to **Figure 2**.

Figure S3. Indole does not apparently influence aminoglycoside entry and resistance in *V. cholerae* WT and *ΔraiA*. A. Intracellular level of neomycin coupled to the fluorophore Cy5 measured by fluorescence associated flow cytometry. Error bars represent standard deviation. **B.** Minimal inhibitory concentrations of tobramycin (TOB) and gentamicin (GEN) measured using *etests* in *V. cholerae*, in the absence (MH) and presence of indole (IND), and indicated in µg/ml by a numeral on each image. Related to **Figure 2**.

Figure S4. Fluorescence detection from the *raiA* promoter-*gfp* fusion by flow cytometry. Representative acquisitions are shown. Each plot represents one experiment. Each experiment was performed at least 3 times and data and statistical significance are shown in the histograms in the main manuscript. **A**: histogram curves: GFP fluorescence is represented in the x-axis (FITC channel), the y-axis represents the number of events corresponding to the number of cells, normalized to height (same number of total cells for both conditions). **B**: dot plots: Bacterial cells' size and shape (rugosity). FSC: forward scatter. SSC: size scatter. The SSC (size scatter) vs FSC (forward scatter) graphs show the distribution of cells by size and shape and no major difference in cell size/shape is observed between the WT and mutants with or without indole. Related to **Figure 4**.

Figure S5. RaiA is involved in persistence in *V. cholerae* and *E. coli*. A. Increase of surviving colonies (persisters) after 20 hours of treatment with tobramycin (TOB) 10 µg/ml (ratio over WT surviving colonies) in *V. cholerae.* Error bars represent geometric standard deviation **B**. Persistence of *E. coli* WT and *raiA* mutant, at late exponential phase (OD 620nm 0.5), after 20 hours treatment with 10 µg/ml tobramycin (TOB) in MH media. Serial dilutions are spotted on plates for estimation of survival. Spot assays were performed at least 3 times. Related to **Figure 2.**

Figure S6. Influence of RaiA on the length of lag phase upon growth restart after the stationary phase. A. Experimental set-up. Repression was achieved with 1% glucose (GLC), induction was achieved with 0.2% arabinose (ARA). **B.** Lag time (minutes) defined as time to reach OD 620 nm 0.15 in WT *V. cholerae* carrying empty vector (p0) or pBAD-RaiA vector (see ABCD in Figure 6). **C.** Lag time (in minutes) defined as time to reach OD 620 nm 0.15 in *V. cholerae* Δ*raiA,* Δ*rmf and* Δ*hpf* and WT *V. cholerae* carrying empty vector (p0) or hibernation factors (pRaiA, pRmf, pHpf) (Figure 7AB) **D**. Lag time (in minutes) defined as time to reach OD 620 nm 0.15 in WT *P. aeruginosa* (Figure 9A) carrying empty vector (p0) or pBAD-RaiA vector. Experiments were performed in triplicates and statistical analysis was performed (**: *p<0.01; ***: p<0.001; ****: p<0.0001;* ns: not significant). Related to **Figure 6, 7AB** and **9A.**

Figure S7. Influence of RaiA, Rmf and Hpf on persistence. Persistence of *V. cholerae* WT and mutants in early exponential phase, after 20 hours treatment with 10 µg/ml tobramycin (TOB) in MH media.

Serial dilutions are spotted on plates for estimation of survival. Spot assays were performed at least 3 times. Related to **Figure 7**

Figure S8. Expression of *gfp* from constitutive promoter (Pc) in conditions where expression from the *raiA* promoter is up or down-regulated. Fluorescence quantification of GFP expression from constitutive promoter by flow cytometry in MH media in exponential phase, in WT and indicated *V. cholerae* deletion mutants. IND: indole (350 µM), DP: 2,2'-Dipyridyl (500 µM). The Y axis represents fluorescence ratio of the mutant over wild type (WT) strain. Error bars represent standard deviation. Related to **Figure 4**.

References

Agafonov, D.E., Kolb, V.A., Nazimov, I.V., and Spirin, A.S. (1999). A protein residing at the subunit interface of the bacterial ribosome. Proc Natl Acad Sci U S A *96*, 12345-12349.

Agafonov, D.E., Kolb, V.A., and Spirin, A.S. (2001). Ribosome-associated protein that inhibits translation at the aminoacyl-tRNA binding stage. EMBO Rep *2*, 399-402.

Andersson, D.I., and Hughes, D. (2014). Microbiological effects of sublethal levels of antibiotics. Nat Rev Microbiol *12*, 465-478.

Baharoglu, Z., Babosan, A., and Mazel, D. (2014). Identification of genes involved in low aminoglycoside-induced SOS response in Vibrio cholerae: a role for transcription stalling and Mfd helicase. Nucleic Acids Res *42*, 2366-2379.

Baharoglu, Z., Bikard, D., and Mazel, D. (2010). Conjugative DNA transfer induces the bacterial SOS response and promotes antibiotic resistance development through integron activation. PLoS Genet *6*, e1001165.

Baharoglu, Z., Krin, E., and Mazel, D. (2013). RpoS Plays a Central Role in the SOS Induction by Sub-Lethal Aminoglycoside Concentrations in Vibrio cholerae. Plos Genetics *9*.

Baharoglu, Z., and Mazel, D. (2011). Vibrio cholerae Triggers SOS and Mutagenesis in Response to a Wide Range of Antibiotics: a Route towards Multiresistance. Antimicrobial Agents and Chemotherapy *55*, 2438-2441.

Basu, A., and Yap, M.N. (2017). Disassembly of the Staphylococcus aureus hibernating 100S ribosome by an evolutionarily conserved GTPase. Proc Natl Acad Sci U S A *114*, E8165-E8173.

Blair, J.M.A., Cloeckaert, A., Nishino, K., and Piddock, L.J.V. (2013). Alternative explanation for indole-induced antibiotic tolerance in Salmonella. P Natl Acad Sci USA *110*, E4569-E4569.

Botsford, J.L., and DeMoss, R.D. (1971). Catabolite repression of tryptophanase in Escherichia coli. J Bacteriol *105*, 303-312.

Brauner, A., Fridman, O., Gefen, O., and Balaban, N.Q. (2016). Distinguishing between resistance, tolerance and persistence to antibiotic treatment. Nat Rev Microbiol *14*, 320-330.

Bray, M.S., Lenz, T.K., Haynes, J.W., Bowman, J.C., Petrov, A.S., Reddi, A.R., Hud, N.V., Williams, L.D., and Glass, J.B. (2018). Multiple prebiotic metals mediate translation. Proc Natl Acad Sci U S A *115*, 12164-12169.

Chant, E.L., and Summers, D.K. (2007). Indole signalling contributes to the stable maintenance of Escherichia coli multicopy plasmids. Mol Microbiol *63*, 35-43.

Chimerel, C., Field, C.M., Pinero-Fernandez, S., Keyser, U.F., and Summers, D.K. (2012). Indole prevents Escherichia coli cell division by modulating membrane potential. Biochim Biophys Acta *1818*, 1590-1594.

Condon, C., Liveris, D., Squires, C., Schwartz, I., and Squires, C.L. (1995). rRNA operon multiplicity in Escherichia coli and the physiological implications of rrn inactivation. J Bacteriol *177*, 4152-4156.

Davies, B.W., Bogard, R.W., and Mekalanos, J.J. (2011). Mapping the regulon of Vibrio cholerae ferric uptake regulator expands its known network of gene regulation. Proc Natl Acad Sci U S A *108*, 12467-12472.

741 Davies, J., Spiegelman, G.B., and Yim, G. (2006). The world of subinhibitory antibiotic concentrations.
742 Curr Opin Microbiol *9*, 445-453.
743 Davis, B.D. (1987). Mechanism of bactericidal action of aminoglycosides. Microbiol Rev *51*, 341-350.
744 Di Pietro, F., Brandi, A., Dzeladini, N., Fabbretti, A., Carzaniga, T., Piersimoni, L., Pon, C.L., and
745 Giuliodori, A.M. (2013). Role of the ribosome-associated protein PY in the cold-shock response of
746 Escherichia coli. Microbiologyopen *2*, 293-307.
747 Espinosa, E., Daniel, S., Hernandez, S.B., Goudin, A., Cava, F., Barre, F.X., and Galli, E. (2020). L-
748 arabinose induces the formation of viable non-proliferating spheroplasts in Vibrio cholerae. Appl
749 Environ Microbiol.
750 Evans, W.C., Richard, W., Handley, C., and Happold, F.C. (1941). The tryptophanase-indole reaction:
751 Some observations on the production of tryptophanase by Esch. coli; in particular the effect of the
752 presence of glucose and amino acids on the formation of tryptophanase. Biochem J *35*, 207-212.
753 Feaga, H.A., Kopylov, M., Kim, J.K., Jovanovic, M., and Dworkin, J. (2020). Ribosome Dimerization
754 Protects the Small Subunit. J Bacteriol *202*.
755 Fraimow, H.S., Greenman, J.B., Leviton, I.M., Dougherty, T.J., and Miller, M.H. (1991). Tobramycin
756 uptake in Escherichia coli is driven by either electrical potential or ATP. J Bacteriol *173*, 2800-2808.
757 Franken, L.E., Oostergetel, G.T., Pijning, T., Puri, P., Arkhipova, V., Boekema, E.J., Poolman, B., and
758 Guskov, A. (2017). A general mechanism of ribosome dimerization revealed by single-particle cryo-
759 electron microscopy. Nature communications *8*, 722.
760 Giuliodori, A.M. (2016). Cold-shock response in Escherichia coli: A model system to study post-
761 transcriptional regulation. In Stress and Environmental Regulation of Gene Expression and
762 Adaptation in Bacteria, F.J. de Bruijn, ed. (Wiley Blackwell: Hoboken), pp. 859–872.
763 Giuliodori, A.M., Brandi, A., Giangrossi, M., Gualerzi, C.O., and Pon, C.L. (2007). Cold-stress-induced
764 de novo expression of infC and role of IF3 in cold-shock translational bias. RNA *13*, 1355-1365.
765 Gohara, D.W., and Yap, M.F. (2018). Survival of the drowsiest: the hibernating 100S ribosome in
766 bacterial stress management. Curr Genet *64*, 753-760.
767 Gualerzi, C.O., Giuliodori, A.M., Brandi, A., Di Pietro, F., Piersimoni, L., Fabbretti, A., and Pon, C.L.
768 (2011). Translation initiation at the root of the cold-shock translational bias. In Ribosomes: Structure,
769 Function, and Dynamics, pp. 143-154.
770 Gutierrez, A., Laureti, L., Crussard, S., Abida, H., Rodriguez-Rojas, A., Blazquez, J., Baharoglu, Z.,
771 Mazel, D., Darfeuille, F., Vogel, J.*, et al.* (2013). beta-lactam antibiotics promote bacterial
772 mutagenesis via an RpoS-mediated reduction in replication fidelity. Nature communications *4*, 1610.
773 Han, T.H., Lee, J.H., Cho, M.H., Wood, T.K., and Lee, J. (2011). Environmental factors affecting indole
774 production in Escherichia coli. Res Microbiol *162*, 108-116.
775 Herisse, M., Duverger, Y., Martin-Verstraete, I., Barras, F., and Ezraty, B. (2017). Silver potentiates
776 aminoglycoside toxicity by enhancing their uptake. Mol Microbiol *105*, 115-126.
777 Hirakawa, H., Inazumi, Y., Masaki, T., Hirata, T., and Yamaguchi, A. (2005). Indole induces the
778 expression of multidrug exporter genes in Escherichia coli. Mol Microbiol *55*, 1113-1126.
779 Hossain, T., Deter, H.S., Peters, E.J., and Butzin, N.C. (2021). Antibiotic tolerance, persistence, and
780 resistance of the evolved minimal cell, Mycoplasma mycoides JCVI-Syn3B. iScience *24*, 102391.
781 Howard, M.F., Bina, X.R., and Bina, J.E. (2019). Indole inhibits ToxR regulon expression in Vibrio
782 cholerae. Infect Immun.
783 Hu, Y., Kwan, B.W., Osbourne, D.O., Benedik, M.J., and Wood, T.K. (2015). Toxin YafQ increases
784 persister cell formation by reducing indole signalling. Environ Microbiol *17*, 1275-1285.
785 Janosi, L., Hara, H., Zhang, S., and Kaji, A. (1996). Ribosome recycling by ribosome recycling factor
786 (RRF)--an important but overlooked step of protein biosynthesis. Adv Biophys *32*, 121-201.
787 Kim, J.S., Yamasaki, R., Song, S., Zhang, W., and Wood, T.K. (2018). Single cell observations show
788 persister cells wake based on ribosome content. Environ Microbiol *20*, 2085-2098.
789 Kobayashi, A., Hirakawa, H., Hirata, T., Nishino, K., and Yamaguchi, A. (2006). Growth phase-
790 dependent expression of drug exporters in Escherichia coli and its contribution to drug tolerance. J
791 Bacteriol *188*, 5693-5703.

Koeva, M., Gutu, A.D., Hebert, W., Wager, J.D., Yonker, L.M., O'Toole, G.A., Ausubel, F.M., Moskowitz, S.M., and Joseph-McCarthy, D. (2017). An Antipersister Strategy for Treatment of Chronic Pseudomonas aeruginosa Infections. Antimicrob Agents Chemother *61*.
Kralj, J.M., Hochbaum, D.R., Douglass, A.D., and Cohen, A.E. (2011). Electrical spiking in Escherichia coli probed with a fluorescent voltage-indicating protein. Science *333*, 345-348.
Krin, E., Pierle, S.A., Sismeiro, O., Jagla, B., Dillies, M.A., Varet, H., Irazoki, O., Campoy, S., Rouy, Z., Cruveiller, S.*, et al.* (2018). Expansion of the SOS regulon of Vibrio cholerae through extensive transcriptome analysis and experimental validation. BMC Genomics *19*, 373.
Lee, H.H., Molla, M.N., Cantor, C.R., and Collins, J.J. (2010). Bacterial charity work leads to population-wide resistance. Nature *467*, 82-85.
Lee, J., Jayaraman, A., and Wood, T.K. (2007). Indole is an inter-species biofilm signal mediated by SdiA. BMC Microbiol *7*, 42.
Lee, J., Zhang, X.S., Hegde, M., Bentley, W.E., Jayaraman, A., and Wood, T.K. (2008). Indole cell signaling occurs primarily at low temperatures in Escherichia coli. ISME J *2*, 1007-1023.
Lee, J.H., and Lee, J. (2010). Indole as an intercellular signal in microbial communities. FEMS Microbiol Rev *34*, 426-444.
Lee, J.H., Wood, T.K., and Lee, J. (2015). Roles of indole as an interspecies and interkingdom signaling molecule. Trends Microbiol *23*, 707-718.
Lelong, C., Aguiluz, K., Luche, S., Kuhn, L., Garin, J., Rabilloud, T., and Geiselmann, J. (2007). The Crl-RpoS regulon of Escherichia coli. Mol Cell Proteomics *6*, 648-659.
Li, Y., Cole, K., and Altman, S. (2003). The effect of a single, temperature-sensitive mutation on global gene expression in Escherichia coli. RNA *9*, 518-532.
Li, Y., Sharma, M.R., Koripella, R.K., Yang, Y., Kaushal, P.S., Lin, Q., Wade, J.T., Gray, T.A., Derbyshire, K.M., Agrawal, R.K.*, et al.* (2018). Zinc depletion induces ribosome hibernation in mycobacteria. Proc Natl Acad Sci U S A *115*, 8191-8196.
Liu, X., Beyhan, S., Lim, B., Linington, R.G., and Yildiz, F.H. (2010). Identification and characterization of a phosphodiesterase that inversely regulates motility and biofilm formation in Vibrio cholerae. J Bacteriol *192*, 4541-4552.
Lo Scrudato, M., and Blokesch, M. (2012). The regulatory network of natural competence and transformation of Vibrio cholerae. PLoS Genet *8*, e1002778.
Maki, Y., Yoshida, H., and Wada, A. (2000). Two proteins, YfiA and YhbH, associated with resting ribosomes in stationary phase Escherichia coli. Genes Cells *5*, 965-974.
Manneh-Roussel, J., Haycocks, J.R.J., Magan, A., Perez-Soto, N., Voelz, K., Camilli, A., Krachler, A.M., and Grainger, D.C. (2018). cAMP Receptor Protein Controls Vibrio cholerae Gene Expression in Response to Host Colonization. MBio *9*.
Martino, P.D., Fursy, R., Bret, L., Sundararaju, B., and Phillips, R.S. (2003). Indole can act as an extracellular signal to regulate biofilm formation of Escherichia coli and other indole-producing bacteria. Canadian journal of microbiology *49*, 443-449.
Matzov, D., Bashan, A., Yap, M.F., and Yonath, A. (2019). Stress response as implemented by hibernating ribosomes: a structural overview. FEBS J *286*, 3558-3565.
McKay, S.L., and Portnoy, D.A. (2015). Ribosome hibernation facilitates tolerance of stationary-phase bacteria to aminoglycosides. Antimicrob Agents Chemother *59*, 6992-6999.
Mehi, O., Bogos, B., Csorgo, B., Pal, F., Nyerges, A., Papp, B., and Pal, C. (2014). Perturbation of iron homeostasis promotes the evolution of antibiotic resistance. Mol Biol Evol *31*, 2793-2804.
Mey, A.R., Wyckoff, E.E., Kanukurthy, V., Fisher, C.R., and Payne, S.M. (2005). Iron and fur regulation in Vibrio cholerae and the role of fur in virulence. Infect Immun *73*, 8167-8178.
Mitchell, S.A. (2009). Indole adsorption to a lipid monolayer studied by optical second harmonic generation. J Phys Chem B *113*, 10693-10707.
Mueller, R.S., Beyhan, S., Saini, S.G., Yildiz, F.H., and Bartlett, D.H. (2009). Indole acts as an extracellular cue regulating gene expression in Vibrio cholerae. J Bacteriol *191*, 3504-3516.

Negro, V., Krin, E., Aguilar Pierle, S., Chaze, T., Giai Gianetto, Q., Kennedy, S.P., Matondo, M., Mazel, D., and Baharoglu, Z. (2019). RadD Contributes to R-Loop Avoidance in Sub-MIC Tobramycin. MBio *10*.
Newton, W.A., and Snell, E.E. (1965). Formation and Interrelationships of Tryptophanase and Tryptophan Synthetases in Escherichia Coli. J Bacteriol *89*, 355-364.
Nikaido, E., Giraud, E., Baucheron, S., Yamasaki, S., Wiedemann, A., Okamoto, K., Takagi, T., Yamaguchi, A., Cloeckaert, A., and Nishino, K. (2012). Effects of indole on drug resistance and virulence of Salmonella enterica serovar Typhimurium revealed by genome-wide analyses. Gut Pathog *4*, 5.
Niven, G.W. (2004). Ribosome modulation factor protects Escherichia coli during heat stress, but this may not be dependent on ribosome dimerisation. Arch Microbiol *182*, 60-66.
Okuda, M. (2015). Mechanism of action of a class of antibiotics from their entry to their target in bacteria : a real time visualization (Université Paris Sud - Paris XI).
Opatowski, M., Tuppin, P., Cosker, K., Touat, M., De Lagasnerie, G., Guillemot, D., Salomon, J., Brun-Buisson, C., and Watier, L. (2019). Hospitalisations with infections related to antimicrobial-resistant bacteria from the French nationwide hospital discharge database, 2016. Epidemiol Infect *147*, e144.
Paranjape, S.S., and Shashidhar, R. (2019). Inhibition of protein synthesis eradicates persister cells of V. cholerae. 3 Biotech *9*, 380.
Pinero-Fernandez, S., Chimerel, C., Keyser, U.F., and Summers, D.K. (2011). Indole transport across Escherichia coli membranes. J Bacteriol *193*, 1793-1798.
Polikanov, Y.S., Blaha, G.M., and Steitz, T.A. (2012). How hibernation factors RMF, HPF, and YfiA turn off protein synthesis. Science *336*, 915-918.
Pontes, M.H., and Groisman, E.A. (2019). Slow growth determines nonheritable antibiotic resistance in Salmonella enterica. Sci Signal *12*.
Prossliner, T., Skovbo Winther, K., Sorensen, M.A., and Gerdes, K. (2018). Ribosome Hibernation. Annu Rev Genet *52*, 321-348.
Prossliner, T., Sorensen, M.A., and Winther, K.S. (2021). Hibernation factors directly block ribonucleases from entering the ribosome in response to starvation. Nucleic Acids Res *49*, 2226-2239.
Puri, P., Eckhardt, T.H., Franken, L.E., Fusetti, F., Stuart, M.C., Boekema, E.J., Kuipers, O.P., Kok, J., and Poolman, B. (2014). Lactococcus lactis YfiA is necessary and sufficient for ribosome dimerization. Mol Microbiol *91*, 394-407.
Qin, D., and Fredrick, K. (2013). Analysis of polysomes from bacteria. Methods Enzymol *530*, 159-172.
Sabeti Azad, M., Okuda, M., Cyrenne, M., Bourge, M., Heck, M.P., Yoshizawa, S., and Fourmy, D. (2020). Fluorescent aminoglycoside antibiotics and methods for accurately monitoring uptake by bacteria. ACS Infect Dis.
Sabharwal, D., Song, T., Papenfort, K., and Wai, S.N. (2015). The VrrA sRNA controls a stationary phase survival factor Vrp of Vibrio cholerae. RNA Biol *12*, 186-196.
Saint-Ruf, C., Garfa-Traore, M., Collin, V., Cordier, C., Franceschi, C., and Matic, I. (2014). Massive diversification in aging colonies of Escherichia coli. J Bacteriol *196*, 3059-3073.
Shimada, T., Yoshida, H., and Ishihama, A. (2013). Involvement of cyclic AMP receptor protein in regulation of the rmf gene encoding the ribosome modulation factor in Escherichia coli. J Bacteriol *195*, 2212-2219.
Slamti, L., Livny, J., and Waldor, M.K. (2007). Global gene expression and phenotypic analysis of a Vibrio cholerae rpoH deletion mutant. J Bacteriol *189*, 351-362.
Soini, J., Ukkonen, K., and Neubauer, P. (2008). High cell density media for Escherichia coli are generally designed for aerobic cultivations - consequences for large-scale bioprocesses and shake flask cultures. Microb Cell Fact *7*, 26.
Song, S., and Wood, T.K. (2020). ppGpp ribosome dimerization model for bacterial persister formation and resuscitation. Biochem Biophys Res Commun.

892 Spoering, A.L., and Lewis, K. (2001). Biofilms and planktonic cells of Pseudomonas aeruginosa have
893 similar resistance to killing by antimicrobials. J Bacteriol *183*, 6746-6751.
894 Taber, H.W., Mueller, J.P., Miller, P.F., and Arrow, A.S. (1987). Bacterial uptake of aminoglycoside
895 antibiotics. Microbiol Rev *51*, 439-457.
896 Tkachenko, A.G., Kashevarova, N.M., Tyuleneva, E.A., and Shumkov, M.S. (2017). Stationary-phase
897 genes upregulated by polyamines are responsible for the formation of Escherichia coli persister cells
898 tolerant to netilmicin. FEMS Microbiol Lett *364*.
899 Touat, M., Opatowski, M., Brun-Buisson, C., Cosker, K., Guillemot, D., Salomon, J., Tuppin, P., de
900 Lagasnerie, G., and Watier, L. (2019). A Payer Perspective of the Hospital Inpatient Additional Care
901 Costs of Antimicrobial Resistance in France: A Matched Case-Control Study. Appl Health Econ Health
902 Policy *17*, 381-389.
903 Ueta, M., Wada, C., Daifuku, T., Sako, Y., Bessho, Y., Kitamura, A., Ohniwa, R.L., Morikawa, K.,
904 Yoshida, H., Kato, T.*, et al.* (2013). Conservation of two distinct types of 100S ribosome in bacteria.
905 Genes Cells *18*, 554-574.
906 Ueta, M., Yoshida, H., Wada, C., Baba, T., Mori, H., and Wada, A. (2005). Ribosome binding proteins
907 YhbH and YfiA have opposite functions during 100S formation in the stationary phase of Escherichia
908 coli. Genes Cells *10*, 1103-1112.
909 Vega, N.M., Allison, K.R., Khalil, A.S., and Collins, J.J. (2012). Signaling-mediated bacterial persister
910 formation. Nat Chem Biol *8*, 431-433.
911 Vega, N.M., Allison, K.R., Samuels, A.N., Klempner, M.S., and Collins, J.J. (2013). Salmonella
912 typhimurium intercepts Escherichia coli signaling to enhance antibiotic tolerance. Proc Natl Acad Sci
913 U S A.
914 Vila-Sanjurjo, A., Schuwirth, B.S., Hau, C.W., and Cate, J.H. (2004). Structural basis for the control of
915 translation initiation during stress. Nature structural & molecular biology *11*, 1054-1059.
916 Wada, A., Mikkola, R., Kurland, C.G., and Ishihama, A. (2000). Growth phase-coupled changes of the
917 ribosome profile in natural isolates and laboratory strains of Escherichia coli. J Bacteriol *182*, 2893-
918 2899.
919 Wang, D., Ding, X., and Rather, P.N. (2001). Indole can act as an extracellular signal in Escherichia coli.
920 J Bacteriol *183*, 4210-4216.
921 Wood, T.K., and Song, S. (2020). Forming and waking dormant cells: The ppGpp ribosome
922 dimerization persister model. Biofilm *2*, 100018.
923 Wood, W.N., Mohler, K., Rinehart, J., and Ibba, M. (2021). Deacylated tRNA Accumulation Is a Trigger
924 for Bacterial Antibiotic Persistence Independent of the Stringent Response. mBio, e0113221.
925 Yamagishi, M., Matsushima, H., Wada, A., Sakagami, M., Fujita, N., and Ishihama, A. (1993).
926 Regulation of the Escherichia coli rmf gene encoding the ribosome modulation factor: growth phase-
927 and growth rate-dependent control. EMBO J *12*, 625-630.
928 Yanofsky, C., Horn, V., and Gollnick, P. (1991). Physiological studies of tryptophan transport and
929 tryptophanase operon induction in Escherichia coli. J Bacteriol *173*, 6009-6017.
930 Zarkan, A., Matuszewska, M., Trigg, S.B., Zhang, M., Belgami, D., Croft, C., Liu, J., El-Ouisi, S.,
931 Greenhalgh, J., Duboff, J.S.*, et al.* (2020). Inhibition of indole production increases the activity of
932 quinolone antibiotics against E. coli persisters. Scientific reports *10*, 11742.
933 Zinskie, J.A., Ghosh, A., Trainor, B.M., Shedlovskiy, D., Pestov, D.G., and Shcherbik, N. (2018). Iron-
934 dependent cleavage of ribosomal RNA during oxidative stress in the yeast Saccharomyces cerevisiae.
935 J Biol Chem *293*, 14237-14248.

936

937

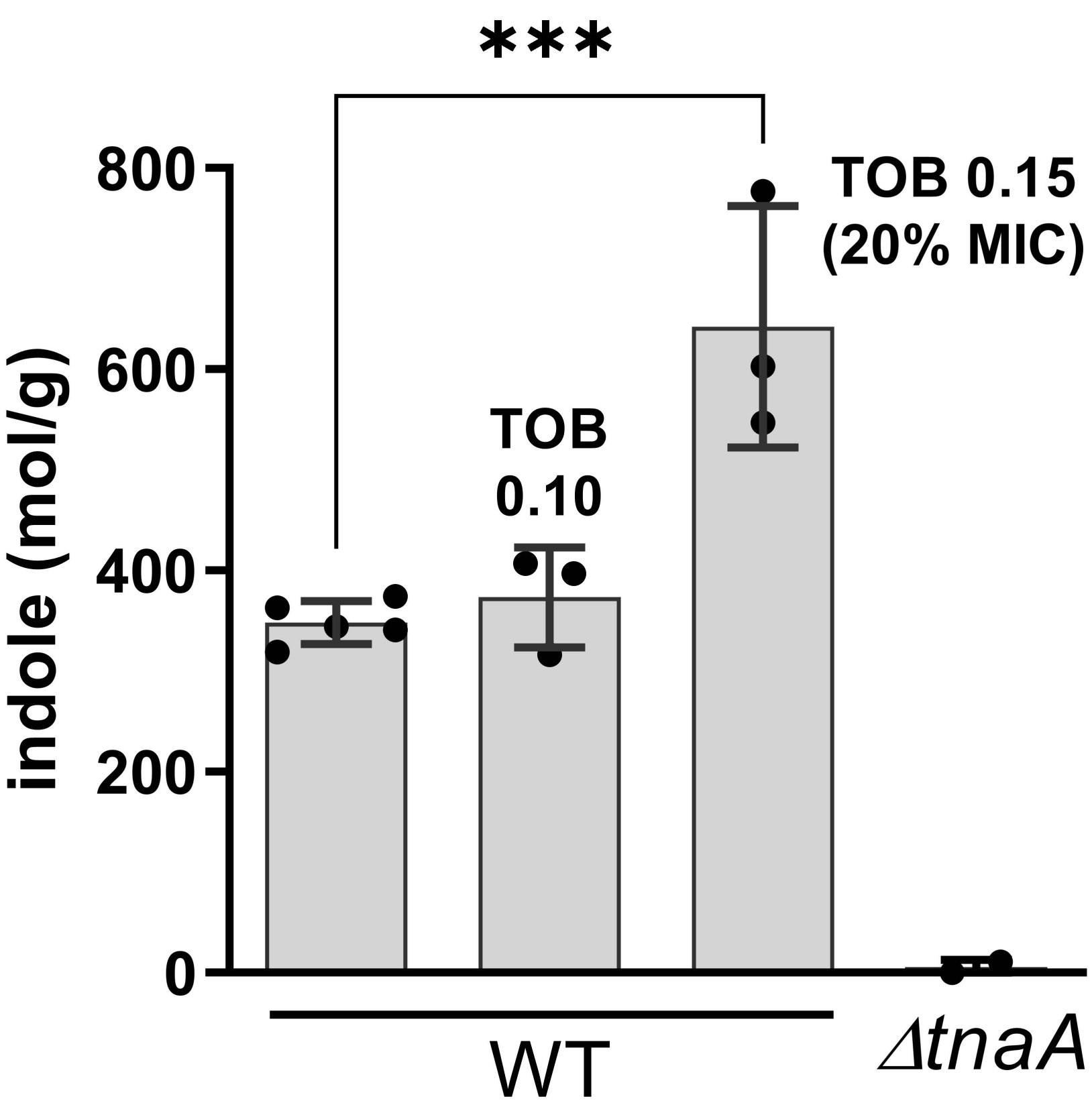
***
800
600
400
200
0
indole (mol/g)
TOB 0.15
(20% MIC)
TOB
0.10
WT
ΔtnaA

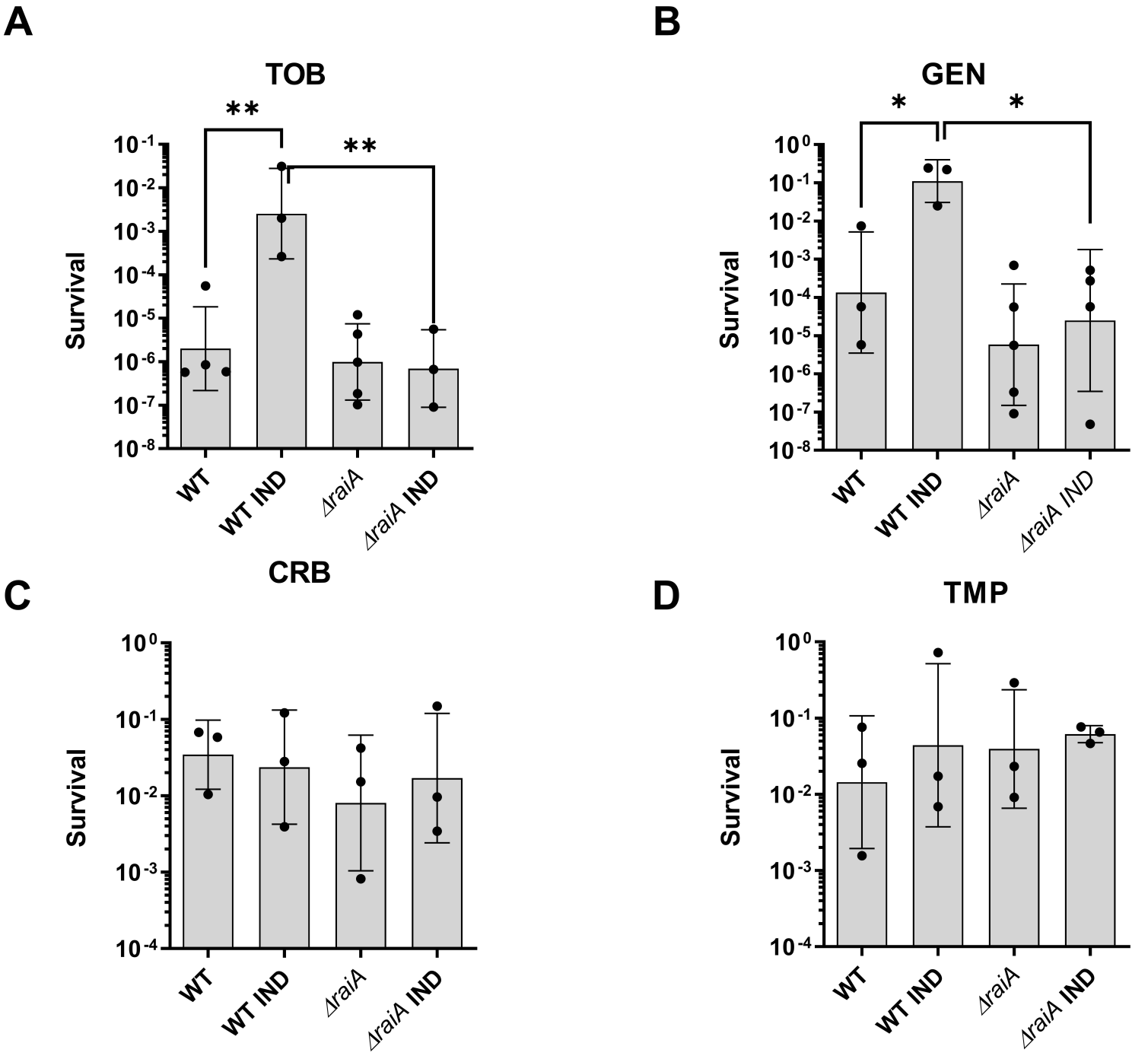
A
TOB
**
**
Survival
10^{-1}
10^{-2}
10^{-3}
10^{-4}
10^{-5}
10^{-6}
10^{-7}
10^{-8}
WT
WT IND
ΔraiA
ΔraiA IND
B
GEN
*
*
Survival
10^{0}
10^{-1}
10^{-2}
10^{-3}
10^{-4}
10^{-5}
10^{-6}
10^{-7}
10^{-8}
WT
WT IND
ΔraiA
ΔraiA IND
C
CRB
Survival
10^{0}
10^{-1}
10^{-2}
10^{-3}
10^{-4}
WT
WT IND
ΔraiA
ΔraiA IND
D
TMP
Survival
10^{0}
10^{-1}
10^{-2}
10^{-3}
10^{-4}
WT
WT IND
ΔraiA
ΔraiA IND

A

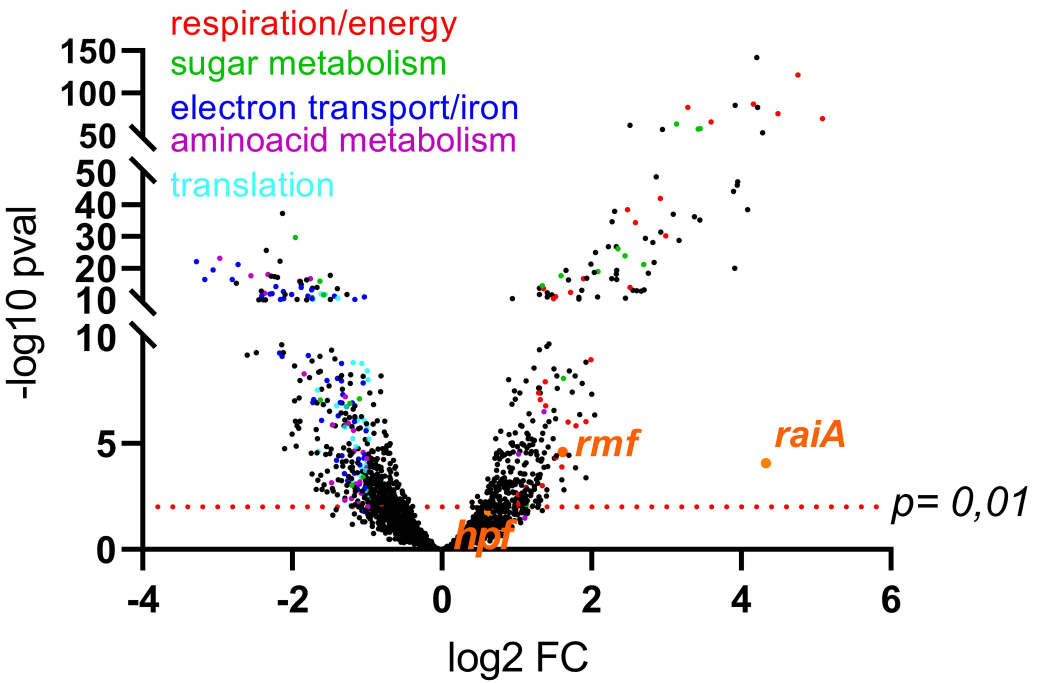
respiration/energy
sugar metabolism
electron transport/iron
aminoacid metabolism
translation
-log10 pval
150
100
50
50
40
30
20
10
10
5
0
-4
-2
0
2
4
6
log2 FC
rmf
raiA
hpf
p= 0,01

B

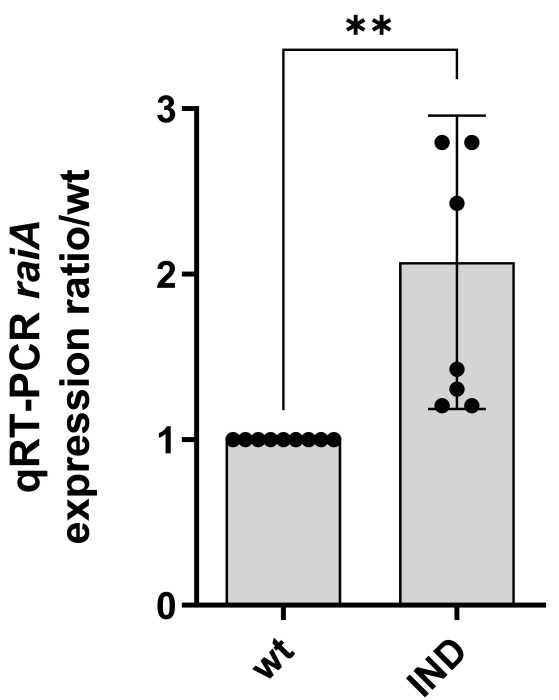
**
qRT-PCR raiA
expression ratio/wt
3
2
1
0
wt
IND

A

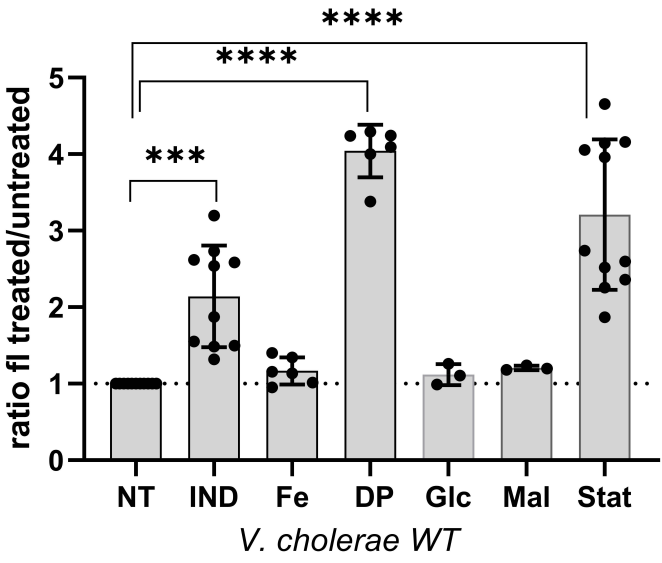
****
****
***
ratio fl treated/untreated
5
4
3
2
1
0
NT
IND
Fe
DP
Glc
Mal
Stat
V. cholerae WT

B

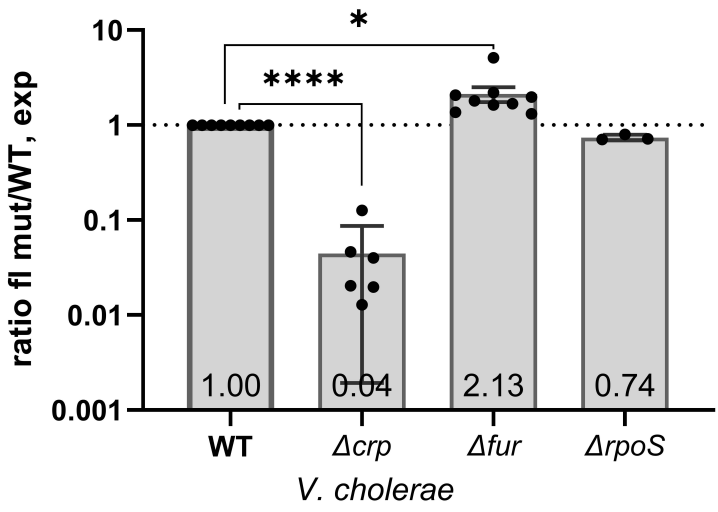
*
****
ratio fl mut/WT, exp
10
1
0.1
0.01
0.001
1.00
0.04
2.13
0.74
WT
Δcrp
Δfur
ΔrpoS
V. cholerae

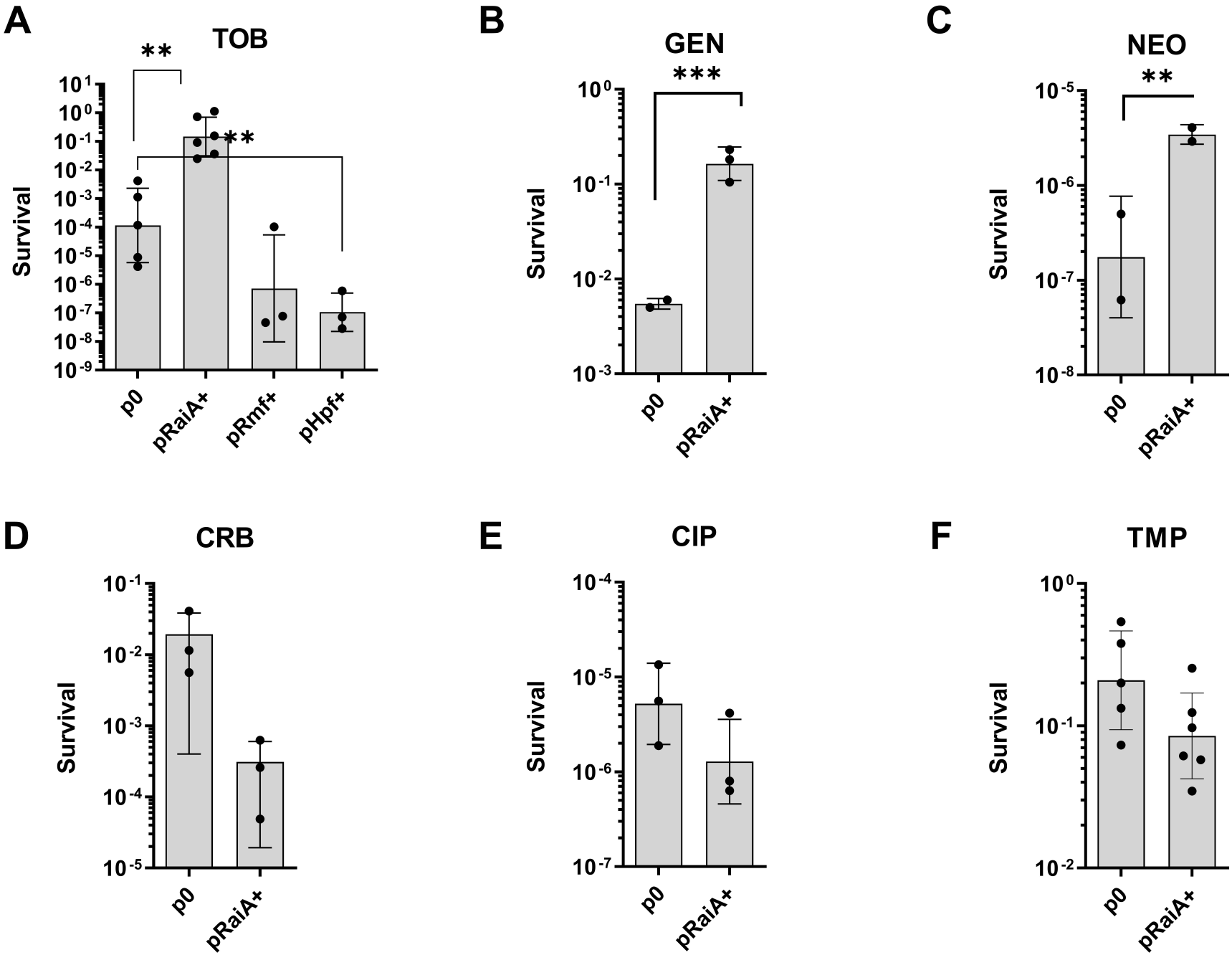
A
TOB
**
**
Survival
p0
pRaiA+
pRmf+
pHpf+
B
GEN
***
Survival
p0
pRaiA+
C
NEO
**
Survival
p0
pRaiA+
D
CRB
Survival
p0
pRaiA+
E
CIP
Survival
p0
pRaiA+
F
TMP
Survival
p0
pRaiA+

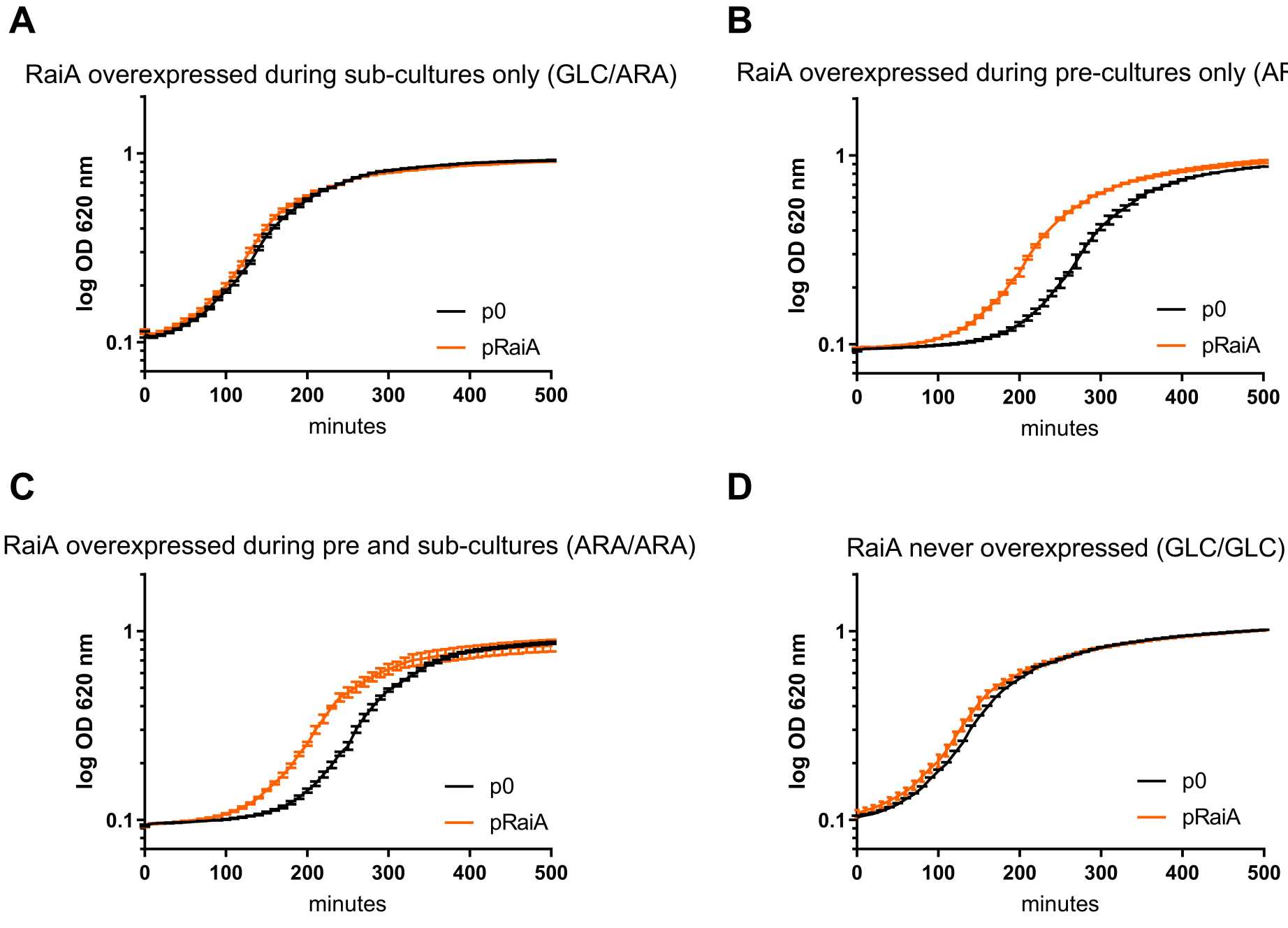
A
RaiA overexpressed during sub-cultures only (GLC/ARA)
log OD 620 nm
1
0.1
0
100
200
300
400
500
minutes
p0
pRaiA
B
RaiA overexpressed during pre-cultures only (ARA/GLC)
log OD 620 nm
1
0.1
0
100
200
300
400
500
minutes
p0
pRaiA
C
RaiA overexpressed during pre and sub-cultures (ARA/ARA)
log OD 620 nm
1
0.1
0
100
200
300
400
500
minutes
p0
pRaiA
D
RaiA never overexpressed (GLC/GLC)
log OD 620 nm
1
0.1
0
100
200
300
400
500
minutes
p0
pRaiA

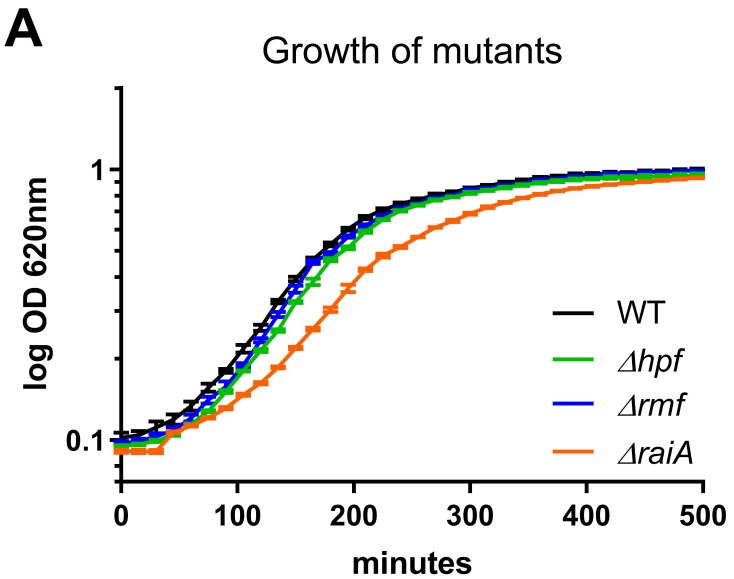
A
Growth of mutants
log OD 620nm
1
0.1
0
100
200
300
400
500
minutes
WT
Δhpf
Δrmf
ΔraiA

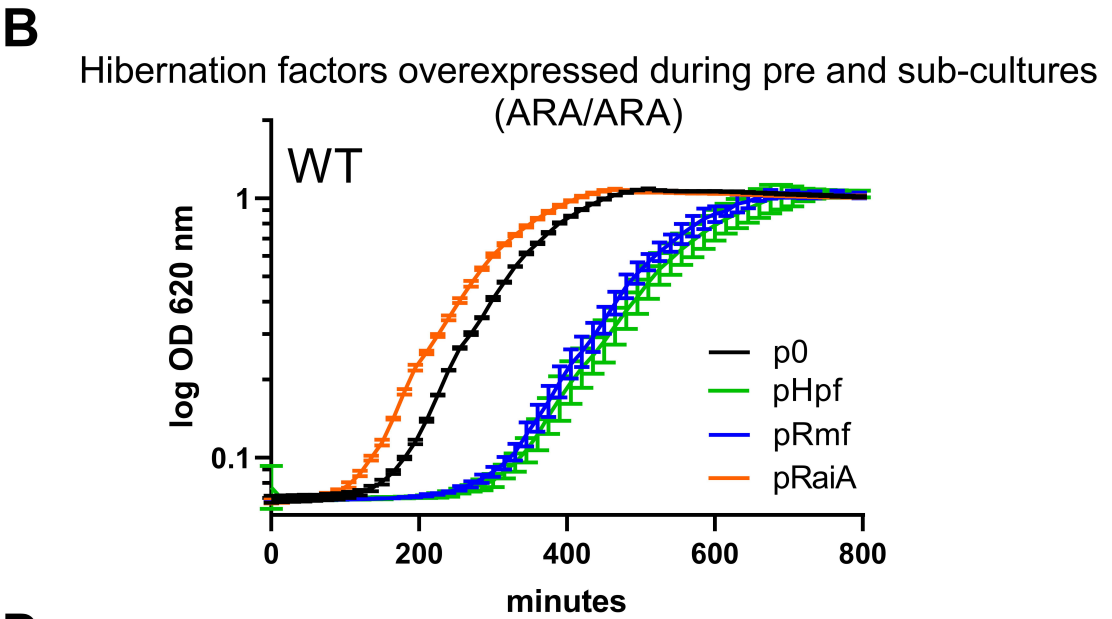
B
Hibernation factors overexpressed during pre and sub-cultures (ARA/ARA)
WT
log OD 620 nm
1
0.1
0
200
400
600
800
minutes
p0
pHpf
pRmf
pRaiA

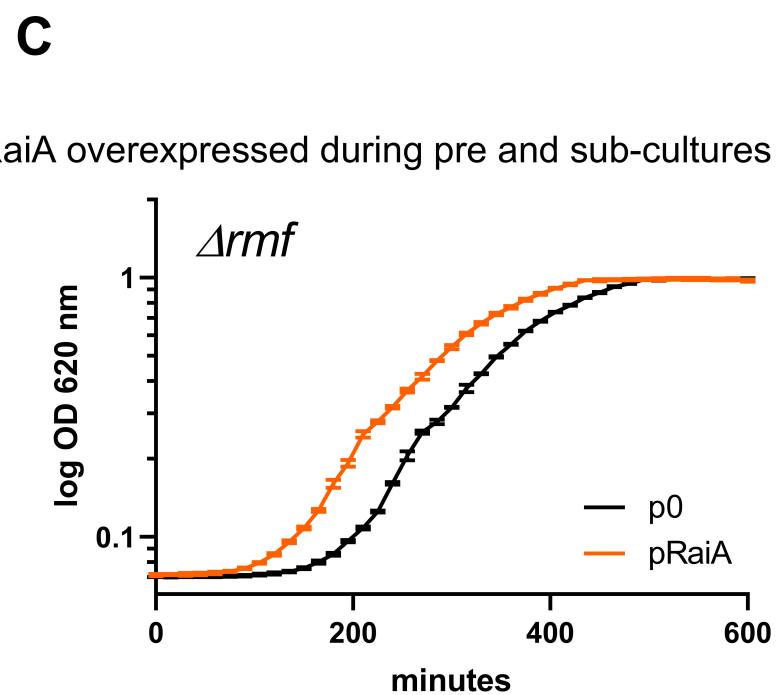
C
RaiA overexpressed during pre and sub-cultures (ARA/ARA)
Δrmf
log OD 620 nm
1
0.1
0
200
400
600
minutes
p0
pRaiA

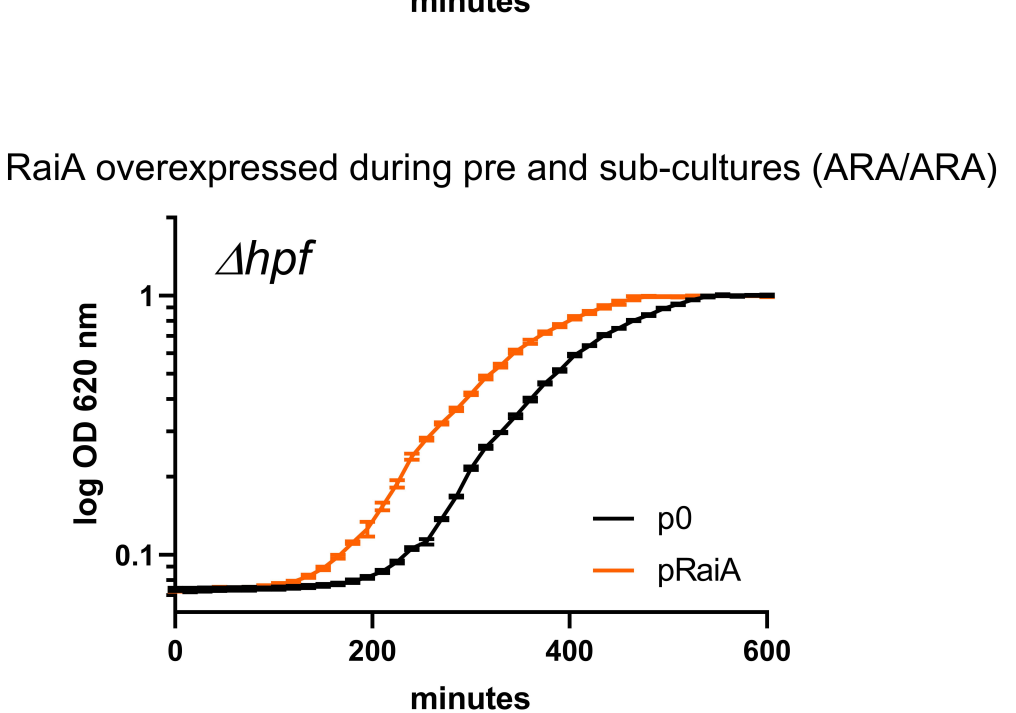
D
RaiA overexpressed during pre and sub-cultures (ARA/ARA)
Δhpf
log OD 620 nm
1
0.1
0
200
400
600
minutes
p0
pRaiA

A

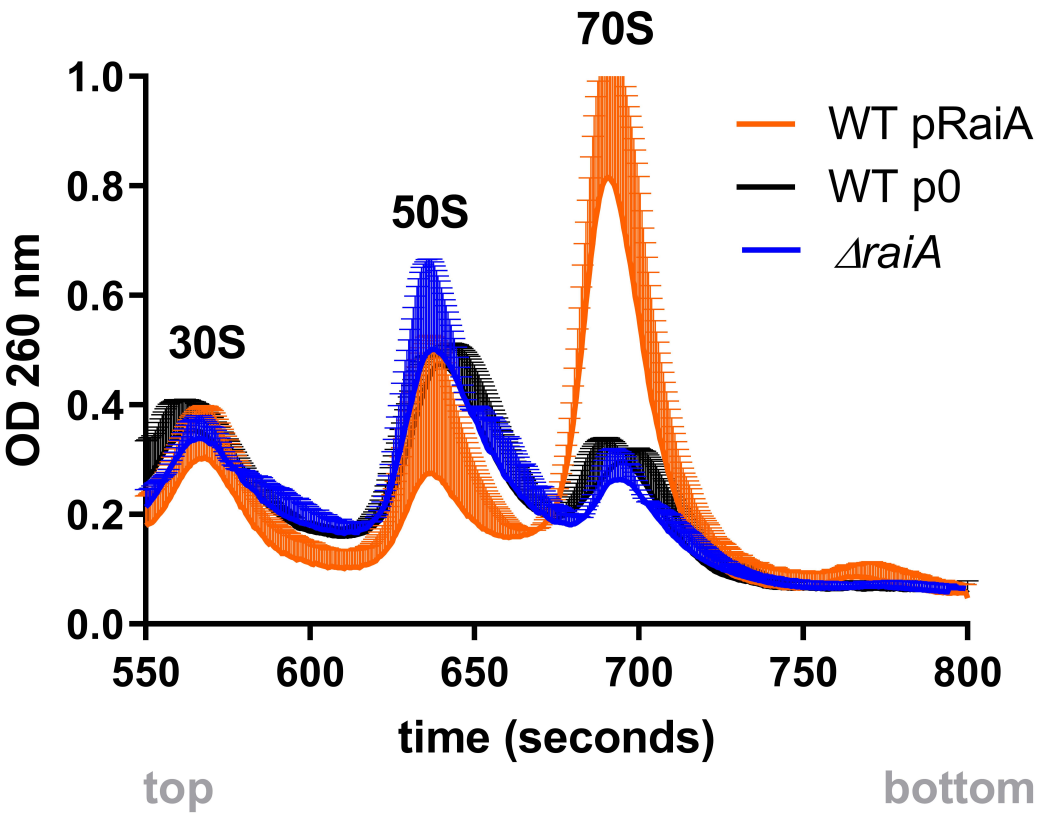
70S
50S
30S
WT pRaiA
WT p0
ΔraiA
OD 260 nm
1.0
0.8
0.6
0.4
0.2
0.0
550
600
650
700
750
800
time (seconds)
top
bottom

B

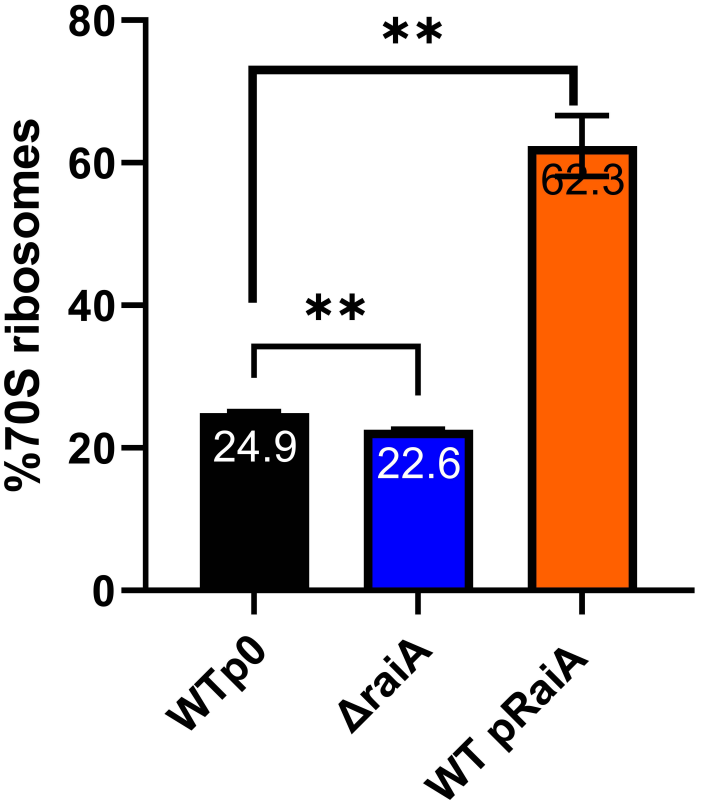
%70S ribosomes
80
60
40
20
0
**
**
24.9
22.6
62.3
WTp0
ΔraiA
WT pRaiA

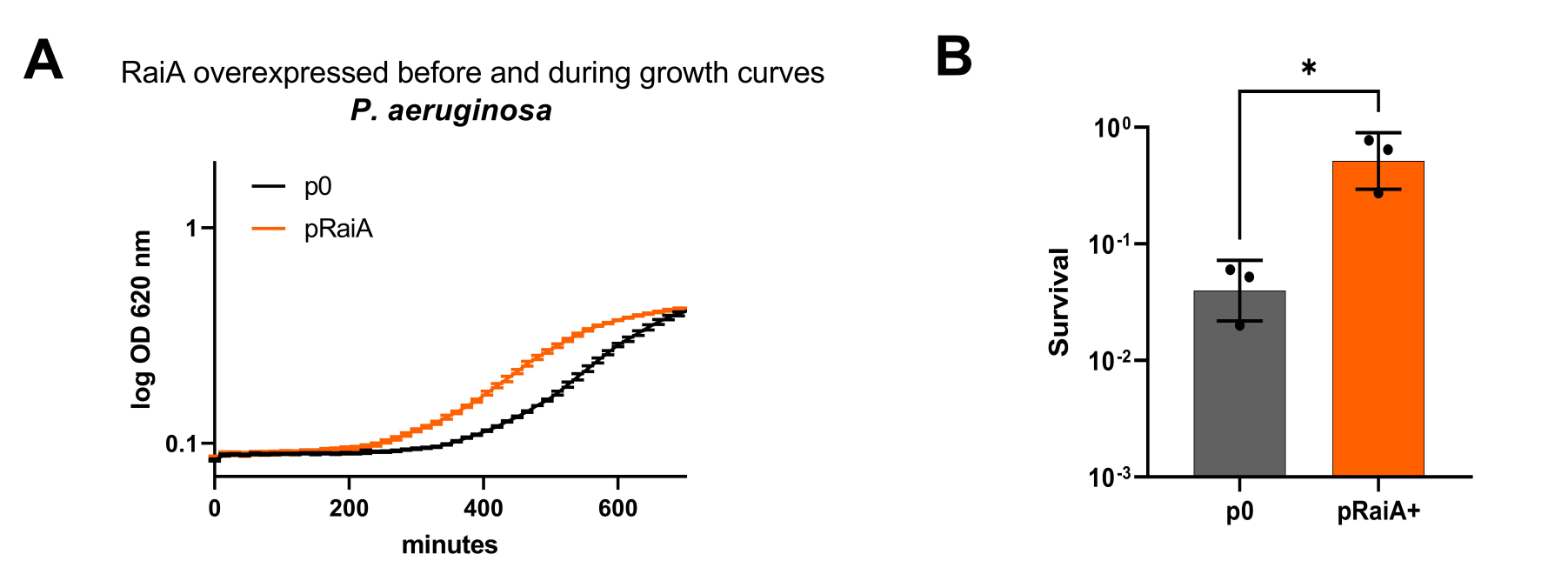
A
RaiA overexpressed before and during growth curves
P. aeruginosa
p0
pRaiA
log OD 620 nm
1
0.1
0
200
400
600
minutes
B
*
Survival
10^0
10^-1
10^-2
10^-3
p0
pRaiA+

A **Persistence**

Impaired translation
AGs>MIC

Translating ribosomes

70S 70S

70S

Non-translating ribosomes

50S 30S 50S 50S 30S 30S 50S 30S

Death

RaiA-bound 70S pool

Sleeping ribosomes

Dissociation
Degradation

Other mechanisms → **Persisters**

e.g. indole + **RaiA induced**

B **Lag period**

Conditions of growth arrest
or non lethal translation stress

Stat phase

Translating ribosomes

70S 70S

70S

Non-translating ribosomes

De novo ribosome synthesis

70S

50S 30S 50S 50S 30S 30S 50S 30S

RaiA-bound 70S pool

Sleeping ribosomes

Faster restart

Dissociation
Degradation

Slower restart

Conditions of growth restart

Figure S1. Indole improves growth of *V. cholerae* in the presence of tobramycin. A. WT**. B.** Δ*raiA*. Growth is measured on a TECAN plate reader. IND: indole 350 µM. TOB: tobramycin sub-MIC (0.6 µg/ml). Experiments were performed in triplicates and geometric means are represented. Error bars represent the geometric standard deviation. Related to **Figure 1**.

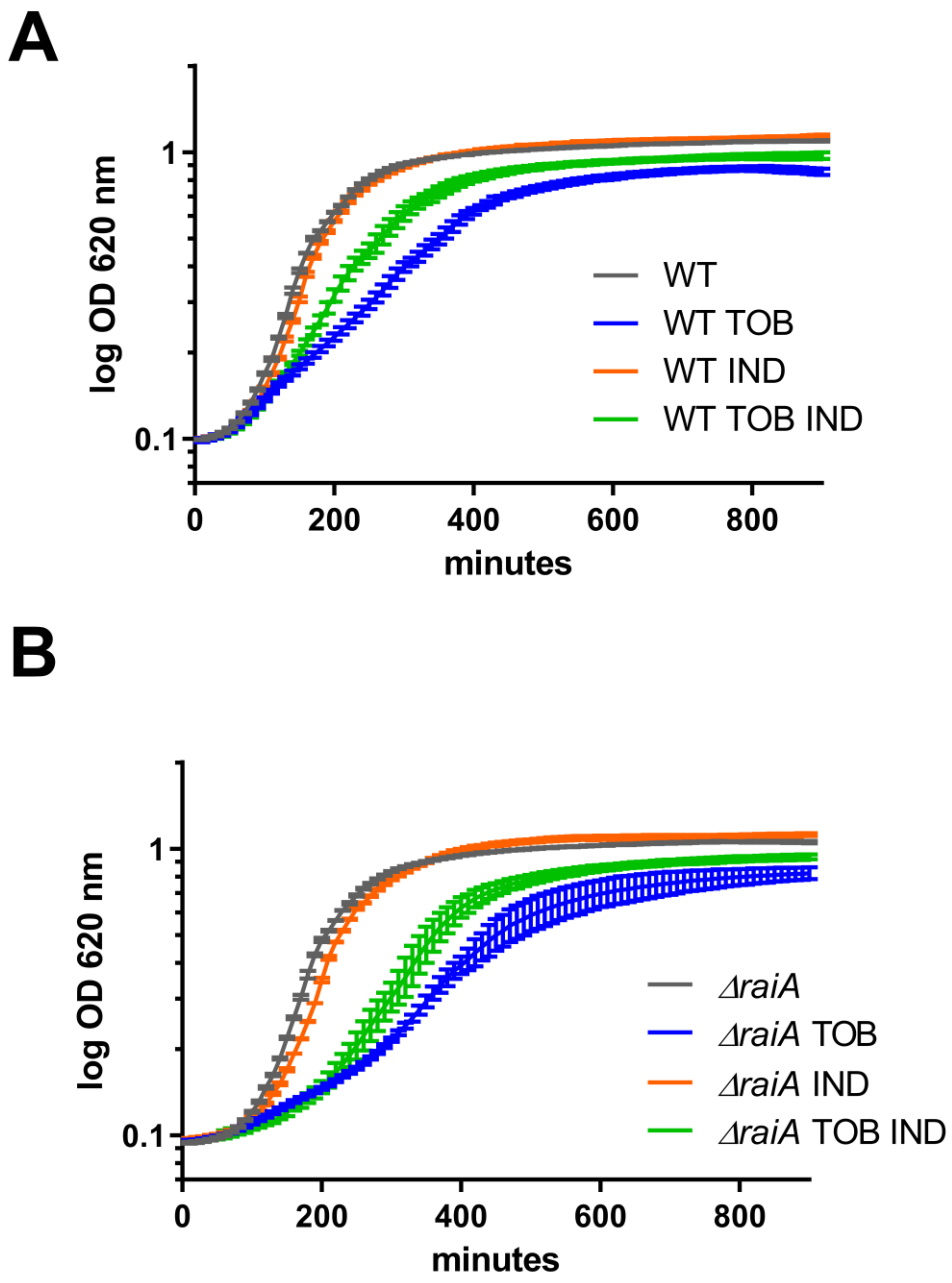

Figure S2. Persistence and the effect of indole. A. Kinetics of survival of WT *V. cholerae* to tobramycin 10 µg/ml in MH media. Time zero corresponds to the total number of CFU before addition of antibiotics, to an early exponential phase culture (OD 620 nm 0.25-0.3), as described in the methods section. The proportion of surviving cells is calculated after plating and counting growing colonies, and is represented for each time point. Curves represent geometric means of at least 3 replicates for each time point and error bars represent geometric standard deviation. **B**. Persistence of *V. cholerae* WT and Δ*tnaA* mutants in exponential phase (in LB instead of MH, to allow indole production, see methods) after 20 hours treatment with specified antibiotics. Tobramycin (TOB): 10 µg/ml, carbenicillin (CRB): 100 µg/ml. Related to **Figure 2**.

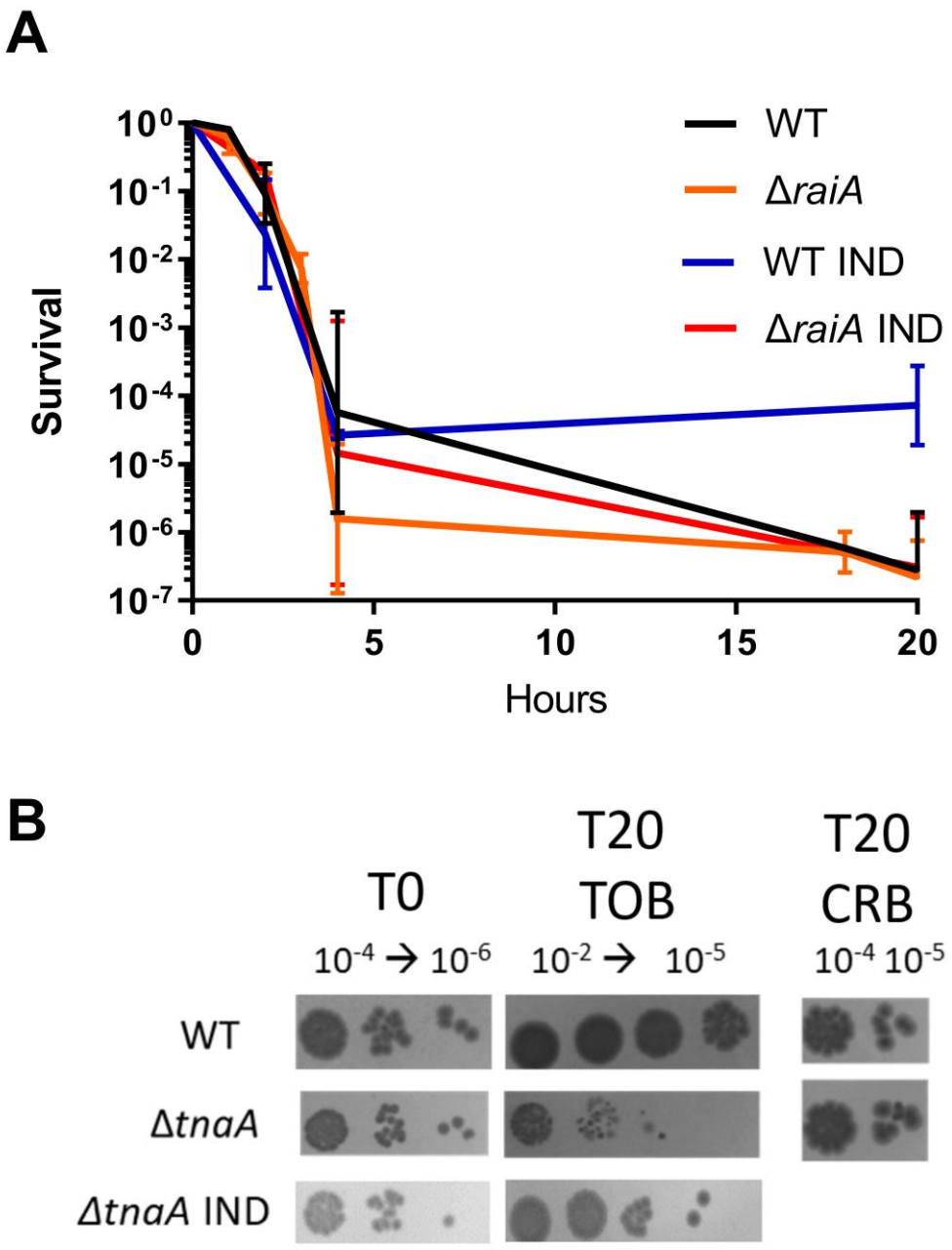

Figure S3. Indole does not apparently influence aminoglycoside entry and resistance in *V. cholerae* WT and Δ*raiA*. A. Intracellular level of neomycin coupled to the fluorophore Cy5 measured by fluorescence associated flow cytometry. Error bars represent standard deviation. **B.** Minimal inhibitory concentrations of tobramycin (TOB) and gentamicin (GEN) measured using *etests* in *V. cholerae*, in the absence (MH) and presence of indole (IND), and indicated in µg/ml by a numeral on each image. Related to **Figure 2**.

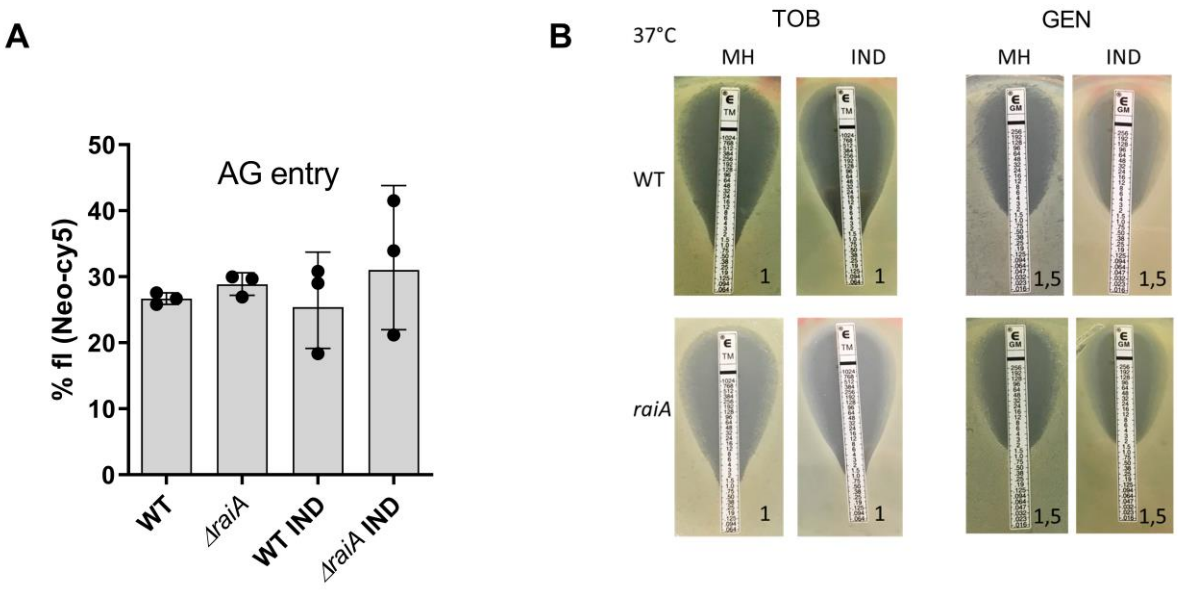

Figure S4. Fluorescence detection from the *raiA* promoter-*gfp* fusion by flow cytometry. Representative acquisitions are shown. Each plot represents one experiment. Each experiment was performed at least 3 times and data and statistical significance are shown in the histograms in the main manuscript. **A**: histogram curves: GFP fluorescence is represented in the x-axis (FITC channel), the y-axis represents the number of events corresponding to the number of cells, normalized to height (same number of total cells for both conditions). **B**: dot plots: Bacterial cells' size and shape (rugosity). FSC: forward scatter. SSC: size scatter. The SSC (size scatter) vs FSC (forward scatter) graphs show the distribution of cells by size and shape and no major difference in cell size/shape is observed between the WT and mutants with or without indole. Related to **Figure 4**.

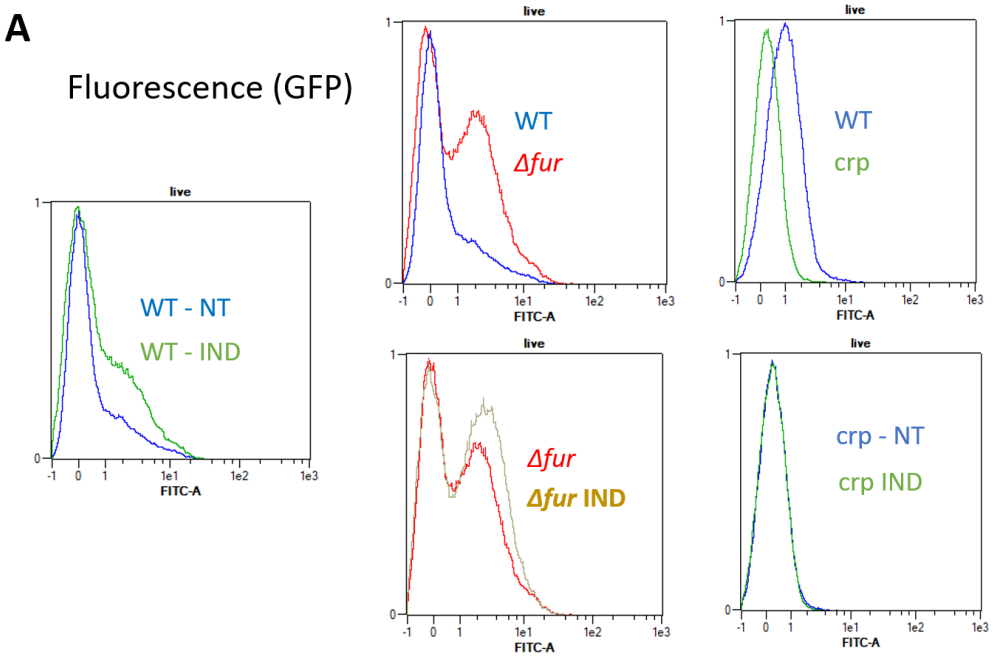

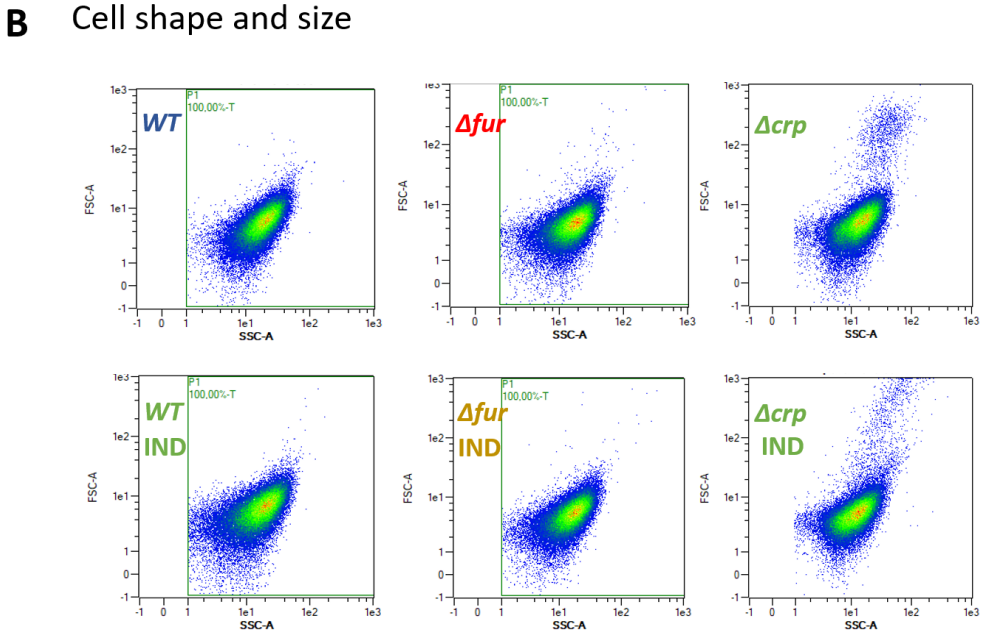

Figure S5. RaiA is involved in persistence in *V. cholerae* and *E. coli*. A. Increase of surviving colonies (persisters) after 20 hours of treatment with tobramycin (TOB) 10 µg/ml (ratio over WT surviving colonies) in *V. cholerae.* Error bars represent geometric standard deviation **B**. Persistence of *E. coli* WT and *raiA* mutant, at late exponential phase (OD 620nm 0.5), after 20 hours treatment with 10 µg/ml tobramycin (TOB) in MH media. Serial dilutions are spotted on plates for estimation of survival. Spot assays were performed at least 3 times. Related to **Figure 2.**

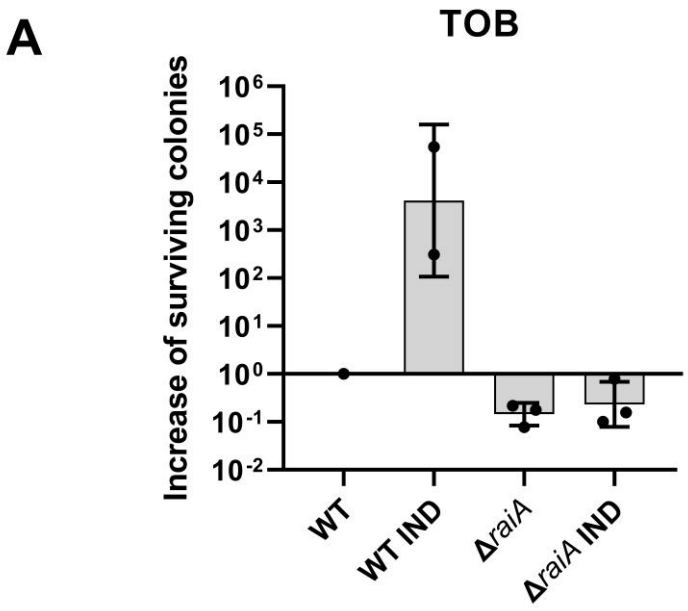

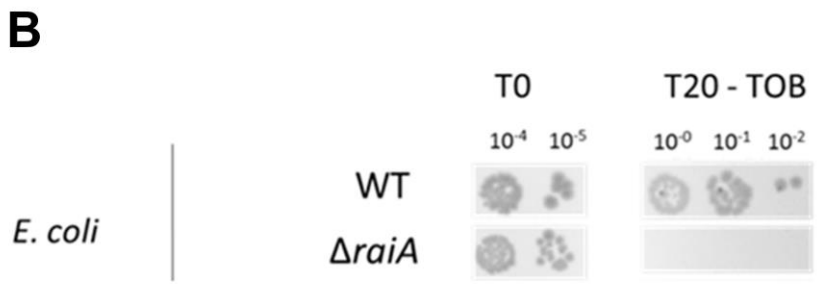

*

Figure S6. Influence of RaiA on the length of lag phase upon growth restart after the stationary phase. A. Experimental set-up. Repression was achieved with 1% glucose (GLC), induction was achieved with 0.2% arabinose (ARA). **B.** Lag time (minutes) defined as time to reach OD 620 nm 0.15 in WT *V. cholerae* carrying empty vector (p0) or pBAD-RaiA vector (see ABCD in Figure 6). **C.** Lag time (in minutes) defined as time to reach OD 620 nm 0.15 in *V. cholerae* Δ*raiA, Δrmf and Δhpf* and WT *V. cholerae* carrying empty vector (p0) or hibernation factors (pRaiA, pRmf, pHpf) (Figure 7AB) **D**. Lag time (in minutes) defined as time to reach OD 620 nm 0.15 in WT *P. aeruginosa* (Figure 9A) carrying empty vector (p0) or pBAD-RaiA vector. Experiments were performed in triplicates and statistical analysis was performed (**: *p<0.01; ***: p<0.001; ****: p<0.0001;* ns: not significant). Related to **Figure 6, 7AB** and **9A.**

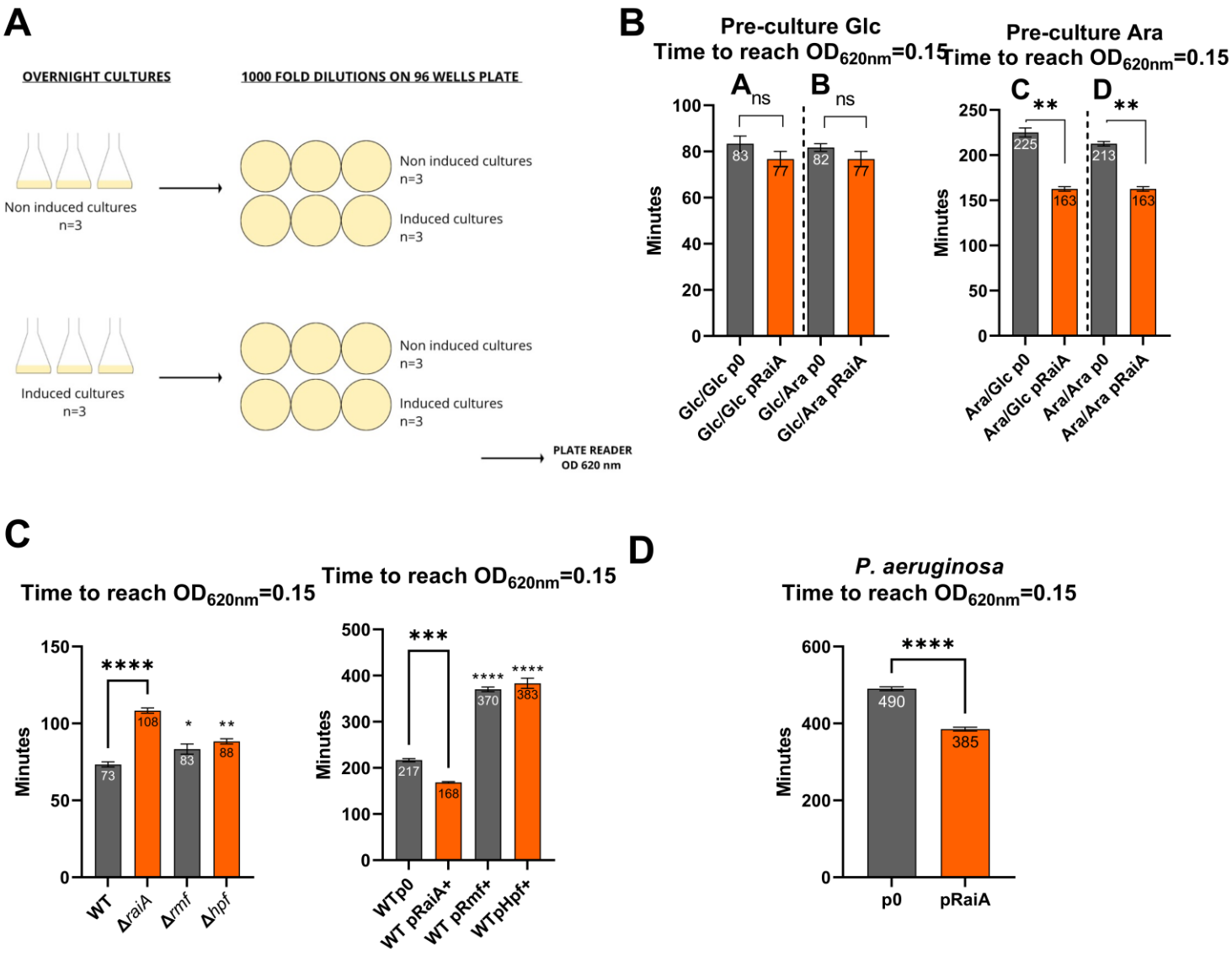

Figure S7. Influence of RaiA, Rmf and Hpf on persistence. Persistence of *V. cholerae* WT and mutants in early exponential phase, after 20 hours treatment with 10 µg/ml tobramycin (TOB) in MH media. Serial dilutions are spotted on plates for estimation of survival. Spot assays were performed at least 3 times. Related to **Figure 7.**

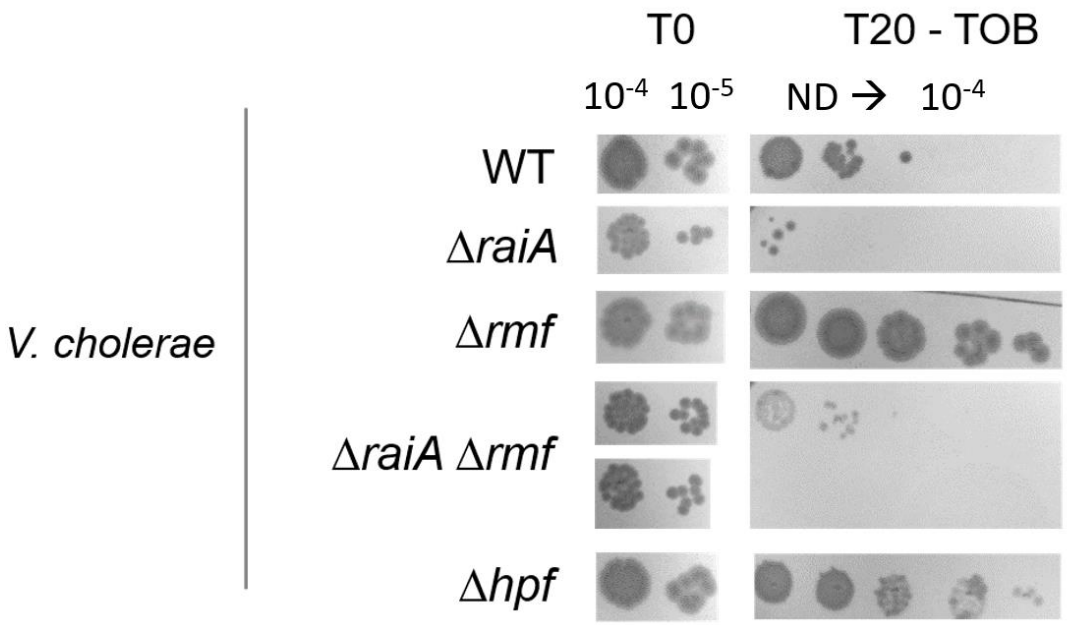

Figure S8. Expression of *gfp* from constitutive promoter (Pc) in conditions where expression from the *raiA* promoter is up or down-regulated. Fluorescence quantification of GFP expression from constitutive promoter by flow cytometry in MH media in exponential phase, in WT and indicated *V. cholerae* deletion mutants. IND: indole (350 µM), DP: 2,2′-Dipyridyl (500 µM). The Y axis represents fluorescence ratio of the mutant over wild type (WT) strain. Error bars represent standard deviation. Related to **Figure 4**.

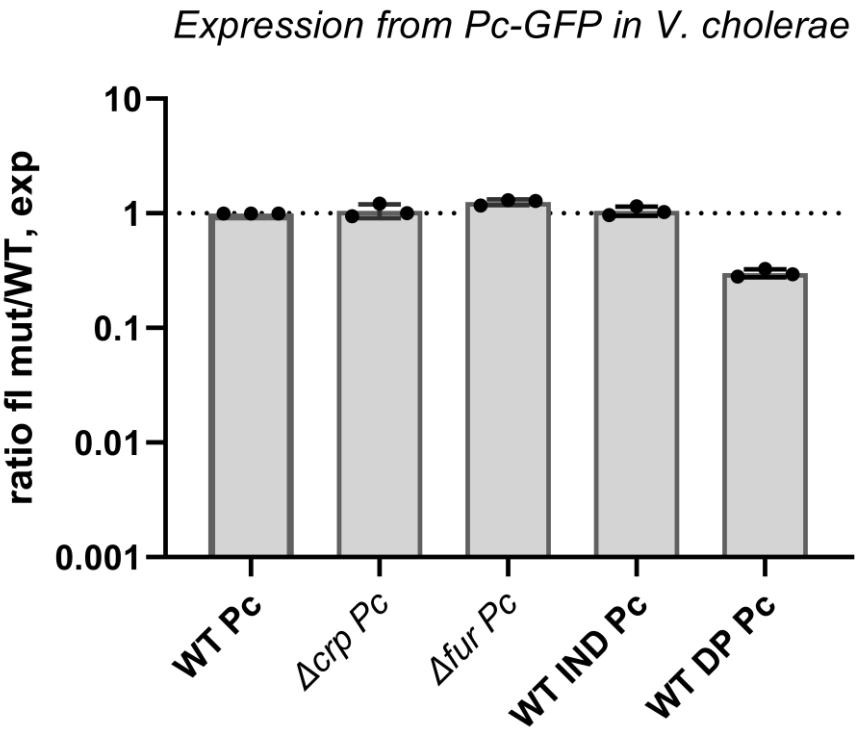

Table S1: **Genes differentially regulated by indole.** Related to **Figure 3.**

Id	norm MH-A	norm MH-B	norm MH-C	norm IND-A	norm IND-B	norm IND-C	**Fold change**	p value	adj p value
UP									
VC0706	3903	4103	3710	80171	68404	145086	20,1	8,0E-03	8,9E-03
VC1484	120	111	142	570	232	501	3,1	2,6E-05	1,3E-01
Motility- Chemotaxis									
VC0410	1779	1337	1477	3761	3910	3890	**2,5**	1,7E-14	8,0E-03
VC1049	413	473	450	2398	2145	2322	**4,9**	1,1E-38	9,0E-03
VC2370	316	270	299	1469	1694	1286	**4,8**	2,6E-35	1,0E-02
VC0414	3748	3638	2441	7061	7532	6276	**2,1**	1,4E-06	1,9E-02
VC0413	658	597	376	1239	1302	1053	**2,1**	1,2E-05	3,0E-02
VC0411	1939	1418	1067	3411	3912	2746	**2,2**	1,6E-05	3,9E-02
VCA0536	508	934	598	1748	2438	2062	**2,9**	6,5E-09	4,6E-02
VCA0954	1750	2718	1721	3886	5756	4105	**2,1**	2,7E-04	5,9E-02
VC0409	9371	6775	5433	26356	19176	30086	**3,3**	3,7E-09	6,3E-02
VC0827	1152	1207	1001	3000	7845	2896	**3,6**	4,4E-07	1,4E-01
VC0826	1967	1966	1336	5009	13957	5414	**4,0**	4,7E-08	1,5E-01
VC1763	428	1057	267	1554	1847	1495	**2,5**	3,3E-03	2,0E-01
VC0820	369	623	278	1133	751	2000	**2,6**	1,5E-03	2,2E-01
Respiration - energy									
VC1115	663	546	508	6006	6126	5482	**9,8**	6,1E-84	7,9E-03
VC0966	7486	7229	6500	15713	18048	21828	**2,6**	2,3E-14	1,1E-02
VC2371	163	157	107	1820	1907	1910	**12,1**	6,9E-67	1,3E-02
VC0477	4301	4841	4095	27291	30017	20290	**5,6**	4,2E-39	1,5E-02
VCA0511	174	249	197	1325	1518	1124	**6,0**	4,6E-35	1,8E-02
VCA0665	329	253	320	9542	8962	8507	**27,0**	5,2E-122	1,8E-02
VCA0665	329	253	320	9542	8962	8507	**27,0**	5,2E-122	1,8E-02
VC1951	347	334	242	5920	6998	5337	**17,9**	1,2E-87	2,0E-02
VC1114	430	337	365	1584	1201	1615	**3,7**	1,7E-17	2,3E-02
VC0356	583	766	592	1725	2375	1675	**2,9**	7,9E-12	2,4E-02
VC2145	931	952	989	7482	9974	5936	**7,6**	1,1E-42	2,4E-02
VCA0563	3532	3857	3297	10041	12683	8503	**2,8**	3,1E-11	2,7E-02
VC2368	8558	11124	8314	25789	18044	26995	**2,4**	4,1E-08	2,9E-02
VC0278	512	493	641	1311	1930	1207	**2,6**	1,2E-08	3,1E-02
VC0485	8659	11085	11206	35439	45566	26147	**3,3**	4,0E-13	3,2E-02
VCA0564	4137	4464	3746	10730	12961	8158	**2,5**	8,6E-08	3,4E-02
VC2656	941	1355	964	33710	22990	28100	**22,5**	2,0E-76	4,1E-02
VC2646	2110	1858	1643	4701	6486	4176	**2,6**	1,7E-07	4,6E-02
VC1687	61	69	112	1751	1301	1331	**15,5**	6,7E-48	5,0E-02

VC1866	7913	12676	7185	81168	101349	63711	**7,9**	6,8E-31	5,3E-02
VC2657	195	285	147	10748	7717	8506	**33,9**	1,1E-70	7,0E-02
VC1516	769	1005	666	2063	981	2137	**2,0**	2,6E-03	7,9E-02
VC2699	895	1117	1191	5749	3169	5283	**4,0**	1,1E-09	9,3E-02
VCA0675	293	225	186	1644	816	2194	**5,7**	1,1E-14	9,5E-02
VC0965	7652	17113	10909	25906	35487	21426	**2,2**	1,2E-03	9,7E-02
VC1513	979	1330	598	4220	2083	4053	**3,2**	9,9E-07	1,0E-01
VC2447	25911	36038	27345	51499	105140	37661	**2,0**	7,0E-03	1,3E-01
VCA0680	583	386	577	2435	870	2782	**3,5**	1,5E-06	1,3E-01
VCA0679	626	383	350	2412	805	2866	**3,8**	9,4E-07	1,6E-01
VCA0678	1612	1152	1434	5851	1605	7354	**3,0**	1,3E-04	1,9E-01
Sugar									
VC2000	33134	38523	32617	94393	96880	78059	**2,5**	2,7E-15	9,0E-03
VC0374	3016	2691	2733	9064	9875	7214	**3,0**	2,5E-18	1,2E-02
VC1973	609	640	690	6655	6173	5216	**8,8**	4,0E-64	1,3E-02
VC1972	229	204	255	2990	2618	2426	**10,7**	3,5E-58	2,0E-02
VC1971	280	208	250	3269	2917	2594	**11,0**	1,4E-58	2,2E-02
VC0487	2056	1941	1773	12473	9768	9035	**5,1**	6,3E-27	2,8E-02
VCA0011	487	642	554	2564	2618	2403	**4,3**	9,8E-20	2,9E-02
VC2689	3011	2941	4636	23493	19880	18705	**5,4**	1,3E-24	3,9E-02
VC2001	1039	618	617	2290	3235	1950	**3,1**	8,4E-09	5,9E-02
VCA0516	258	256	239	1777	2151	1542	**6,5**	7,7E-22	6,0E-02
VCA0013	493	1132	476	2028	1287	1755	**2,2**	7,3E-03	1,7E-01
RRR									
VCA0521	1439	1451	801	3686	3125	3167	**2,6**	3,1E-07	4,4E-02
VCA0520	694	723	482	1449	1115	1411	**2,0**	3,1E-05	2,9E-02
VC2386	4774	8304	2645	8736	6458	24643	**2,2**	3,3E-02	3,6E-01
Metabol									
VC0336	7124	8934	9210	19907	24075	16926	**2,4**	2,8E-09	1,8E-02
VC0026	268	258	311	1582	1606	1262	**5,0**	1,6E-27	2,1E-02
VCA0235	3581	3566	3392	8268	5703	8159	**2,0**	5,8E-05	3,3E-02
VCA0875	2063	2616	1307	5759	4746	4221	**2,4**	7,0E-06	4,4E-02
VC2698	2245	3759	3380	7765	5269	7196	**2,1**	6,6E-04	5,7E-02
VC2373	1415	690	1058	2458	3824	2252	**2,5**	6,8E-05	8,7E-02
VC2361	4108	2170	3027	19721	15393	32664	**6,1**	1,1E-13	1,3E-01
Nucleotide									
VCA0564	4137	4464	3746	10730	12961	8158	**2,5**	8,6E-08	3,4E-02
VC1034	470	448	562	1528	1273	1225	**2,7**	5,9E-13	1,2E-02
regulators									
VC0486	1203	1242	753	11275	8624	10176	**8,5**	1,0E-37	3,6E-02
VC1719	1362	981	674	5308	5146	6057	**5,1**	4,1E-20	4,3E-02
VCA0562	824	717	348	1268	1261	1628	**2,1**	9,6E-04	7,1E-02

VC1919	12704	12883	7383	28846	15905	39769	**2,4**	1,1E-03	1,2E-01
VC2366	483	775	287	1133	1549	946	**2,2**	3,7E-03	1,2E-01
csrD	58131	44933	26252	102802	52169	157915	**2,2**	1,0E-02	1,8E-01
Membrane									
VC1315	54	49	49	1059	987	1071	**18,6**	6,1E-84	1,0E-08
VC2484	2791	2555	2045	8396	7987	7622	**3,2**	4,9E-20	1,1E-02
VC2485	2791	2555	2045	8396	7987	7622	**3,2**	4,9E-21	1,1E-02
VCA0591	531	462	342	1184	1285	1183	**2,7**	9,1E-12	1,6E-02
VC0976	1443	1713	1027	3220	2738	3167	**2,1**	1,4E-05	3,1E-02
VC2149	145	110	144	2554	1821	2827	**15,4**	6,3E-47	5,7E-02
VC0654	606	731	365	2927	5686	3163	**5,9**	8,2E-14	1,1E-01
VCA0628	680	1842	822	2839	1462	4368	**2,2**	1,7E-02	2,9E-01
Others									
VC0652	74	71	98	1343	1362	1262	**15,1**	3,0E-86	1,0E-08
VC0428	523	576	695	4516	4519	4760	**7,3**	1,6E-49	1,6E-02
VC1892	819	567	543	1182	2075	1046	**2,1**	5,6E-04	7,2E-02
VC0037	801	555	621	1749	1301	2937	**2,8**	6,0E-06	8,9E-02
VC1765	1538	4879	1100	7066	10157	6196	**2,6**	3,1E-03	2,9E-01
Hypothetical									
VCA0718	329	301	343	1989	1854	1881	**5,7**	6,9E-63	1,0E-08
VC1865	741	620	752	15085	13445	13011	**18,5**	7,9E-143	7,1E-03
VC1871	630	784	729	5093	6873	5480	**7,7**	7,7E-58	1,3E-02
VC1077	1496	1106	1197	2628	2923	2918	**2,2**	1,1E-08	1,4E-02
VCA0236	299	343	418	1039	1012	978	**2,8**	2,1E-12	1,5E-02
VCA1013	41	54	72	1544	916	1414	**19,5**	9,5E-54	5,0E-02
VCA0741	8417	7150	6445	35536	27576	52687	**4,8**	2,1E-17	5,5E-02
VCA0919	1107	806	959	3604	2763	4638	**3,6**	4,7E-11	5,5E-02
VC0871	209	193	259	1657	1019	2475	**6,8**	3,3E-19	8,0E-02
VC1853	2696	2439	1227	5889	3740	7203	**2,4**	3,1E-04	9,6E-02
VC2035	272	247	652	883	1154	1004	**2,4**	4,9E-04	1,1E-01
VCA0367	870	2025	677	2495	2608	3104	**2,1**	6,6E-03	1,5E-01
VCA0547	1134	821	2003	3510	1518	3735	**2,0**	2,3E-02	1,9E-01
VC1770	338	770	245	1049	1704	933	**2,4**	5,3E-03	2,1E-01
VC2221	97	191	99	3971	1113	3984	**15,1**	9,8E-21	2,4E-01
VCA0283	721	1944	390	2479	2047	3333	**2,2**	1,7E-02	2,6E-01
VC1764	769	2351	507	4476	4878	3997	**3,0**	5,2E-04	2,8E-01
DOWN									
Electron transfer - Ion									
VC2415	6690	8047	8130	1766	1466	1837	0,2	3,9E-40	6,4E-38
VCA0228	703	914	818	60	32	108	0,1	8,9E-25	7,7E-23
VC1265	1746	1306	1376	237	112	243	0,2	8,6E-24	6,8E-22
VCA0227	2696	3888	2205	333	155	375	0,1	4,4E-22	3,3E-20

VCA0230	883	1120	957	128	53	173	0,1	5,5E-19	3,1E-17
VCA0229	545	636	685	68	15	72	0,1	6,8E-19	3,7E-17
VC2559	1531	1298	1238	326	158	308	0,2	1,3E-16	6,1E-15
VC2414	20657	25736	21516	6744	3908	6762	0,3	2,5E-16	1,2E-14
VC1434	5799	4818	6784	1544	2021	1387	0,3	1,6E-15	6,9E-14
VC1544	860	841	702	211	92	200	0,2	5,8E-15	2,3E-13
VC1266	992	730	899	180	81	218	0,2	2,8E-14	1,1E-12
VC1548	828	977	762	200	71	185	0,2	3,5E-14	1,3E-12
VC1168	2427	1657	3276	600	422	657	0,2	4,4E-14	1,6E-12
VC2560	938	837	656	178	57	151	0,2	1,6E-13	5,6E-12
VC0575	3481	4499	4787	1741	1310	1531	0,4	1,7E-13	5,9E-12
VC0540	1091	965	938	257	204	349	0,3	1,9E-13	6,4E-12
VC1890	4135	4112	4697	2193	1882	2160	0,5	2,8E-13	9,2E-12
VC1267	1006	697	951	208	95	240	0,2	1,2E-12	3,6E-11
VC1625	6073	5424	5715	1808	1036	2011	0,3	1,3E-12	3,8E-11
VC1547	1186	1193	907	270	101	276	0,2	2,0E-12	5,9E-11
VC1623	2356	1972	1754	913	895	853	0,4	2,2E-12	6,6E-11
VC0608	1724	3895	2700	607	375	613	0,2	2,0E-11	5,5E-10
VC1543	1647	1544	1204	468	228	484	0,3	2,7E-11	7,1E-10
VC1264	3449	2931	2531	663	257	830	0,2	3,0E-11	7,8E-10
VC0541	2020	1993	2192	759	645	969	0,4	6,9E-11	1,7E-09
VC0627	1608	1342	1589	479	458	718	0,4	3,9E-10	8,7E-09
VC2413	11184	12876	15480	4976	2760	5137	0,3	4,8E-10	1,0E-08
VC0574	4963	6302	6116	2629	1626	2374	0,4	5,1E-10	1,1E-08
VCA0779	1014	1043	1299	573	473	544	0,5	6,7E-10	1,4E-08
VC1425	18728	18568	11818	6031	6511	6308	0,4	2,6E-09	4,9E-08
VC1190	3535	3491	3519	1105	534	1290	0,3	4,7E-09	8,7E-08
VC0539	816	759	978	299	125	291	0,3	5,5E-09	1,0E-07
VC2031	1195	956	1683	516	398	518	0,4	6,3E-09	1,1E-07
VC0538	2463	3016	3026	969	418	946	0,3	6,6E-09	1,2E-07
VC2044	4468	3773	4970	2081	1443	2069	0,4	6,9E-09	1,2E-07
VC1624	2450	2405	2567	1013	552	1133	0,4	3,1E-08	5,0E-07
VC0384	2708	2991	1808	989	444	818	0,3	5,1E-08	8,1E-07
VC1350	1809	1972	2095	700	899	926	0,4	6,0E-08	9,2E-07
VC2099	4134	4299	6134	2367	2308	2392	0,5	1,8E-07	2,5E-06
VC1299	2194	1529	1452	766	807	883	0,5	3,3E-06	3,5E-05
VC2389	12335	10446	14700	5767	2538	5581	0,4	3,7E-06	3,8E-05
VC0168	4710	4663	3918	2115	1538	2593	0,5	5,0E-06	5,0E-05
VC1439	3658	4680	4161	2062	1186	2295	0,5	5,5E-06	5,5E-05
VC0385	2632	2744	1443	910	465	974	0,4	6,3E-06	6,3E-05
VC0386	1716	1717	944	651	435	748	0,4	2,9E-05	2,5E-04
VCA0554	3640	1975	4155	1213	845	1601	0,4	3,1E-05	2,6E-04

VC0731	9328	18667	16354	5035	7322	4748	0,4	7,7E-05	5,8E-04
VC0034	1465	2168	3551	936	1054	1174	0,5	1,2E-04	8,2E-04
VC0573	4031	5106	3159	2130	1225	2439	0,5	1,4E-04	9,8E-04
VC1440	803	1073	578	467	268	424	0,5	1,7E-04	1,1E-03
VCA0907	1430	2408	1943	1139	688	868	0,5	2,0E-04	1,3E-03
VC2089	762	1693	896	567	307	554	0,5	2,2E-04	1,4E-03
VC1441	3956	4982	2505	2010	1104	2188	0,5	3,7E-04	2,2E-03
VCA0496	1389	942	2071	426	1108	411	0,5	4,2E-03	1,6E-02
Sugar metabolism									
VCA0896	3304	3007	3497	889	693	872	0,3	1,6E-32	1,8E-30
VC1126	7293	10250	7992	2766	2625	2583	0,3	2,4E-18	1,2E-16
VCA0657	685	529	732	221	201	201	0,3	7,2E-14	2,5E-12
VC1004	6034	4770	6826	1934	1231	1837	0,3	4,2E-13	1,4E-11
VC2024	3794	3293	4602	1688	1965	1679	0,5	4,2E-09	8,0E-08
VCA0897	3467	2804	1622	845	579	943	0,3	4,9E-09	8,9E-08
VCA0898	5767	4943	6369	2709	1746	2587	0,4	7,2E-09	1,3E-07
VC0910	3175	3395	3392	1601	1326	1539	0,5	1,1E-05	1,0E-04
VC0911	4479	3736	4242	1881	2225	1776	0,5	2,5E-05	2,2E-04
VC2480	1448	1607	2584	982	741	885	0,5	5,1E-05	4,0E-04
VCA1060	2171	771	1674	633	563	664	0,4	1,4E-04	9,5E-04
VC2183	5155	4222	6751	2904	1660	3070	0,5	2,8E-04	1,7E-03
Aminoacid metabolism									
VC1658	2116	1124	2478	185	194	252	0,1	8,2E-26	7,4E-24
VC0008	724	505	822	117	118	140	0,2	1,2E-20	7,9E-19
VC0009	679	385	742	88	83	99	0,2	4,2E-20	2,6E-18
VC0472	6447	7377	9080	2458	1906	2154	0,3	3,0E-19	1,7E-17
VC1312	2358	2539	3364	624	800	669	0,3	1,9E-18	9,8E-17
VC0010	3040	2440	3330	550	251	670	0,2	2,0E-14	7,7E-13
VC0880	758	657	1076	241	122	270	0,3	2,2E-10	5,2E-09
VCA1073	509	701	623	250	182	291	0,4	3,3E-09	6,3E-08
VC0743	6022	4953	6483	2669	1673	2698	0,4	7,6E-08	1,1E-06
VC1995	1199	1731	2309	639	415	724	0,4	8,9E-08	1,3E-06
VCA0815	3885	3098	3980	1836	1216	1630	0,4	1,7E-07	2,4E-06
VC0907	596	504	737	298	182	300	0,4	2,0E-06	2,3E-05
VC0941	10076	7756	8318	4801	2914	4531	0,5	2,3E-06	2,6E-05
VC2682	2219	1588	1853	772	900	1076	0,5	5,2E-06	5,2E-05
VC0947	10671	13096	9872	4646	6635	4962	0,5	1,5E-05	1,4E-04
VCA0772	607	666	968	364	202	431	0,5	8,6E-05	6,4E-04
VC0275	3965	3080	4200	1403	423	1669	0,4	1,0E-04	7,2E-04
VC2485	1370	3351	2132	1019	971	914	0,5	1,1E-04	8,0E-04
VCA0088	2895	3412	2191	1471	647	1654	0,5	3,7E-04	2,2E-03
VC0662	1746	1104	2625	973	890	798	0,5	3,8E-04	2,2E-03

VC0576	3097	3766	9997	1913	2839	1831	0,4	7,3E-04	3,9E-03
VCA0076	970	1503	1188	541	146	612	0,4	9,4E-04	4,8E-03
VC1492	2786	6743	2369	1909	1011	2088	0,5	1,5E-03	6,9E-03
VC2746	19210	29045	38036	10763	19348	10475	0,5	2,3E-03	9,8E-03
Nucleotide metabolism									
VC0276	5517	4824	5808	1963	752	2223	0,3	3,1E-06	3,3E-05
VC0767	8972	9299	12691	4208	4262	4502	0,4	2,4E-10	5,7E-09
VC0768	17636	14237	15989	5714	3303	5613	0,3	1,3E-09	2,7E-08
VC0986	16980	16609	14315	7288	6361	7172	0,4	9,9E-09	1,7E-07
VC1228	2458	2040	2902	784	365	922	0,3	1,6E-07	2,2E-06
VC1721	2424	2857	3565	1020	1480	1120	0,4	3,7E-08	6,0E-07
VC2171	1886	1374	2592	1049	478	1191	0,5	3,2E-03	1,3E-02
VC2227	7683	7434	9542	1542	600	1786	0,2	3,4E-12	9,6E-11
VC2258	5189	4353	6703	2373	3004	1852	0,5	1,3E-06	1,6E-05
VC2277	6821	6135	7227	1701	1908	1914	0,3	1,0E-18	5,3E-17
VC2352	8009	5520	8212	3958	2318	4075	0,5	3,7E-04	2,2E-03
VC2712	6475	3650	5923	2192	772	2789	0,4	7,2E-04	3,8E-03
VCA0607	1153	603	1425	331	773	334	0,5	3,7E-03	1,5E-02
VC1365	972	1192	1204	492	581	539	0,5	5,0E-07	6,5E-06
Translation									
VC0218	57141	36230	62003	25376	23118	26376	0,5	6,6E-06	6,5E-05
VC0291	10456	11726	12645	5607	4153	5227	0,4	6,1E-11	1,5E-09
VC0359	62186	45942	57114	27307	22476	29864	0,5	1,1E-05	1,0E-04
VC0360	65435	46613	78079	26811	25570	27739	0,4	4,5E-07	6,0E-06
VC0361	29304	38455	33303	17321	16307	16634	0,5	4,4E-10	9,8E-09
VC0369	24665	21200	59251	15852	6855	16988	0,4	1,8E-03	8,1E-03
VC0379	793	970	1720	567	485	531	0,5	4,7E-05	3,8E-04
VC0520	15942	19754	24705	6763	8291	6571	0,4	9,5E-09	1,6E-07
VC0570	55026	72405	87623	29769	23007	32471	0,4	1,1E-08	1,9E-07
VC0571	20538	27307	71337	12432	9502	11204	0,3	2,1E-06	2,4E-05
VC0644	1515	1015	1370	552	434	509	0,4	1,3E-09	2,7E-08
VC0645	2212	1491	2617	645	503	659	0,3	2,2E-12	6,5E-11
VC0646	74425	45508	52075	24930	23318	30660	0,5	1,7E-05	1,5E-04
VC0659	4553	4864	6873	1701	1920	1491	0,3	3,0E-14	1,1E-12
VC1209	8390	9867	9418	4451	4396	4138	0,5	6,6E-11	1,7E-09
VC1219	1824	1726	2168	991	864	970	0,5	1,6E-10	3,8E-09
VC1220	4783	4380	6074	2824	2175	2437	0,5	1,4E-07	1,9E-06

VC1297	5980	5708	9049	2891	2950	3392	0,5	5,1E-08	8,1E-07
VC1640	42672	27586	45907	10871	10746	14654	0,3	8,3E-09	1,5E-07
VC1923	14635	30088	14378	9167	11082	8555	0,5	7,1E-04	3,8E-03
VC2025	10223	7808	14105	3020	3736	2634	0,3	1,5E-09	3,0E-08
VC2026	69458	52676	55871	21480	25695	22013	0,4	1,2E-07	1,7E-06
VC2214	6055	7838	8737	3254	3998	2586	0,5	1,1E-06	1,4E-05
VC2259	34754	44090	37821	18907	21812	17310	0,5	4,8E-07	6,2E-06
VC2342	66170	86994	100616	45347	39129	36577	0,5	5,5E-08	8,5E-07
VC2461	2014	1761	2572	814	837	695	0,4	9,0E-13	2,9E-11
VC2579	8782	23257	18636	7681	5267	7624	0,4	7,6E-05	5,7E-04
VC2583	8239	20804	14710	7616	6339	6607	0,5	2,7E-04	1,7E-03
VC2620	1574	1292	1490	785	527	762	0,5	2,2E-05	1,9E-04
VC2664	4009	5269	4052	1503	1695	1142	0,3	4,5E-14	1,6E-12
Others									
csrC2	3606	1920	2667	508	802	551	0,3	9,0E-11	2,2E-09
VIBCH10294	454	271	1091	284	121	291	0,4	5,8E-03	2,1E-02
VC0033	661	587	1321	282	403	265	0,4	1,3E-05	1,2E-04
VC1003	4970	3770	3744	1838	1149	2060	0,4	8,1E-07	1,0E-05
VC1490	685	850	1294	330	344	399	0,4	1,4E-06	1,6E-05
VC1208	3478	4196	5582	2153	1811	1986	0,5	1,4E-07	2,0E-06
VC2460	3572	3075	3149	1084	1300	1026	0,4	2,8E-20	1,8E-18
VC0290	7761	7686	8352	2994	2610	3228	0,4	5,3E-16	2,4E-14
VC2459	960	791	658	428	353	392	0,5	8,0E-08	1,2E-06
VC2647	6843	4552	3914	1936	3109	2207	0,5	1,8E-04	1,2E-03
VC0749	1248	1409	1596	739	601	674	0,5	3,0E-10	6,7E-09
VC0766	1307	1242	3902	984	737	1256	0,5	6,3E-03	2,2E-02
Membrane - transporters									
VC1577	6497	2204	6096	403	1657	363	0,2	1,4E-06	1,7E-05
VC1195	2511	3007	2599	1076	1138	1086	0,4	4,1E-14	1,5E-12
VC1962	1002	693	894	237	323	230	0,3	3,0E-11	7,8E-10
VC1043	20149	34658	22588	7960	8029	9141	0,3	5,1E-09	9,3E-08
VCA0862	718	539	837	239	239	338	0,4	4,9E-08	7,8E-07
VC1655	1156	809	1960	372	425	333	0,3	6,9E-09	1,2E-07
VC1409	885	311	759	79	245	73	0,3	1,1E-06	1,3E-05
VC1329	2576	1202	2399	450	273	641	0,3	5,4E-09	9,9E-08
VC2305	5931	3437	9844	1711	2267	2010	0,3	1,1E-06	1,4E-05
VCA0554	3640	1975	4155	1213	845	1601	0,4	3,1E-05	2,6E-04
VC2278	7821	6452	9648	2026	1781	2313	0,3	3,4E-18	1,7E-16
VC1319	3625	988	2722	474	1989	485	0,5	1,6E-02	4,9E-02
VCA1071	777	918	739	333	197	313	0,4	1,5E-11	4,0E-10

VC1669	764	292	1161	137	223	135	0,3	1,4E-07	1,9E-06
VC0156	13036	12336	11471	2758	7063	2800	0,4	6,7E-05	5,1E-04
VC0475	1465	834	1238	579	468	527	0,5	1,5E-06	1,8E-05
Hypothetical									
VC0268	1534	1816	2463	739	1253	701	0,5	5,3E-04	3,0E-03
VC0519	673932	74591	56109	23575	31849	20968	0,4	1,0E-07	1,5E-06
VC0714	3388	1594	2591	663	2020	811	0,5	8,5E-03	2,9E-02
VC1052	1431	1646	2032	291	395	315	0,2	7,1E-20	4,3E-18
VC1058	762	936	1507	368	638	343	0,5	1,0E-03	5,2E-03
VC1074	639	609	1692	286	317	303	0,3	2,5E-06	2,8E-05
VC1317	4580	788	3907	213	1306	301	0,4	6,8E-03	2,4E-02
VC1574	1767	647	1134	366	505	432	0,4	7,6E-06	7,3E-05
VC1575	786	269	1065	134	207	119	0,3	1,0E-07	1,5E-06
VC1576	2727	1008	1653	330	786	345	0,3	2,5E-06	2,8E-05
VC1578	3800	1491	1767	278	1236	270	0,3	2,3E-04	1,5E-03
VC1832	1010	861	1883	390	605	473	0,4	4,6E-05	3,7E-04
VC1941	3896	3191	4799	1591	1861	1619	0,4	1,5E-08	2,5E-07
VC2093	364	468	980	286	316	262	0,5	1,2E-03	6,0E-03
VC2443	1378	1147	2022	611	768	809	0,5	4,3E-05	3,5E-04
VC2472	1677	1930	2799	671	813	648	0,4	9,3E-10	1,9E-08
VC2706	14791	12371	19055	2652	2846	3038	0,2	2,8E-28	2,8E-26
VCA0026	2034	2585	2667	1005	1465	984	0,5	7,5E-05	5,6E-04
VCA0921	4725	4659	8190	1557	2134	1754	0,3	8,6E-09	1,5E-07
Metabol									
VC0522	4113	2988	3708	1695	2094	1487	0,5	8,2E-07	1,0E-05
VC1942	1302	1679	3645	440	438	455	0,2	2,0E-11	5,3E-10
VC0869	14734	12746	18061	3007	1208	3242	0,2	2,7E-12	7,7E-11
VC1040	977	1202	1356	697	434	627	0,5	8,6E-06	8,3E-05
VCA0150	2635	1976	2642	1116	702	1170	0,4	1,4E-05	1,3E-04
VCA0614	2154	1520	2118	759	457	842	0,4	1,2E-07	1,7E-06
VCA0558	2076	607	4525	607	1460	718	0,5	1,0E-02	3,4E-02
VCA0496	1389	942	2071	426	1108	411	0,5	4,2E-03	1,6E-02
VC0992	1408	1336	1672	627	435	786	0,4	1,1E-07	1,6E-06
VCA0843	1854	2880	1583	839	200	997	0,4	4,7E-04	2,7E-03
VC2545	10175	14016	15506	3639	4482	3767	0,3	1,8E-10	4,4E-09
VC0745	15244	15708	17276	6155	7574	7144	0,4	3,3E-08	5,3E-07
VCA0863	2047	1494	2025	616	561	814	0,4	3,9E-11	1,0E-09
VCA0661	794	886	1062	483	357	513	0,5	2,9E-06	3,1E-05
VC0051	4018	2862	4106	1016	374	1138	0,3	5,6E-08	8,7E-07
VC0052	2282	2082	3109	621	263	597	0,2	8,0E-12	2,2E-10
VC2226	11858	12602	16080	2538	1208	2848	0,2	3,7E-15	1,5E-13

VC1625	6073	5424	5715	1808	1036	2011	0,3	1,3E-12	3,8E-11
VC1738	8039	9711	16080	6283	5005	4652	0,5	4,8E-05	3,8E-04
VC2256	2868	2130	4467	1588	1450	1314	0,5	2,5E-05	2,1E-04

Table S2: Strains and plasmids. Related to STAR Methods.

Strain	Strain number	Construction
Vibrio cholerae		
N16961 wt strain		
N16961 hapR+ wt strain	F606	Gift from Melanie Blokesch
Δ*raiA (VC0706)*	J251	PCR amplification of 500 bp up and down regions of VC0706 using primers ZIP381/384 and ZIP382/383. PCR amplification of *aadA7* conferring spectinomycin resistance on pAM34 using ZB47/48. PCR assembly of the VCA0706::aad7 fragment using ZIP383/384 and allelic exchange by natural transformation, as described previously (Val *et al.*, 2012, Negro *et al.*, 2019)
Δ*rmf (VC1484)*	L557	allelic exchange by integration and excision of conjugative suicide plasmid pMP7 L045, replacing the gene with *frt::aph::frt* as described previously (Val *et al.*, 2012, Negro *et al.*, 2019)
Δ*hpf (VC2530)*	M566	allelic exchange by integration and excision of conjugative suicide plasmid pMP7 M472, replacing the gene with *frt::aph::frt* as described previously (Val *et al.*, 2012, Negro *et al.*, 2019)
Δ*raiA* Δ*rmf*	L790	allelic exchange by integration and excision of conjugative suicide plasmid pMP7 L045 in J251, replacing the gene with *frt::aph::frt* as described previously (Val *et al.*, 2012, Negro *et al.*, 2019)
Δ*crp*	9950	allelic exchange by integration and excision of conjugative suicide plasmid pMP7 8348 , replacing the gene with *aad7* (Val *et al.*, 2012, Negro *et al.*, 2019)
Δ*fur*	N541	allelic exchange by integration and excision of conjugative suicide plasmid pMP7 N450, replacing the gene with *frt::aph::frt* as described previously (Val *et al.*, 2012, Negro *et al.*, 2019)
Δ*rpoS*	A321	Baharoglu *et al., 2013*
Δ*tnaA (VC0161)*	J253	PCR amplification of 500 bp up and down regions of VC0161 using primers ZIP93/94 and ZIP95/96. PCR amplification of *aadA7* conferring spectinomycin resistance on pAM34 using ZIP97/98. PCR assembly of the VCA0161::spec fragment using ZIP93/96 and allelic exchange by natural transformation, as described previously (Val *et al.*, 2012, Negro *et al.*, 2019)
Escherichia coli		
MG1655 wt strain		laboratory collection
Δ*raiA*	J237	P1 transduction from KEIO strain JW2578-1
***Pseudomonas aeruginosa* PAO1**		laboratory collection
Plasmids		
pBAD43		spectinomycin resistant. Carries Para promoter repressed by glucose 1% and induced by arabinose 0.2%. (Guzman, 1995)
pBAD43-RaiA+	L907	*raiA* (VC0706) amplified using primers raiAeco/raiAxba and cloned under Pbad using 5' EcoRI and 3' XbaI restriction sites
pBAD43-Hpf+	M834	*hpf* (VC2530) amplified using primers hpfeco/hpfxba and cloned under Pbad promoter using 5' EcoRI and 3' XbaI restriction sites
pBAD43-Rmf+	M831	*rmf* (VC1484) amplified using primers rmfeco/rmfxba and cloned under Pbad using 5' EcoRI and 3' XbaI restriction sites

pSC101-PraiA-gfp	L707	raiA promoter region (500 bp) was amplified using primers ZIP383/446 and gfp was amplified using primers zip443/444. 2 fragments were assembled by PCR assembly using primers ZIP383/ZIP443, so that *gfp* is fused to the *raiA* promoter at the ATG start codon of *raiA*. The assembled fragment was cloned into pTOPO and extracted using EcoRI and cloned into pSC101 low copy plasmid (carbenicillin resistant).
pSC101-Pc-gfp	N110	gfp was amplified using primers carrying the promoter zip513/200. The fragment was cloned into pTOPO and extracted using EcoRI and cloned into pSC101 low copy plasmid (carbenicillin resistant).
pMP7-∆hpf::kan	M472	gibson assembly using primers MV450/451 for the amplification of pMP7 vector, primers VC2530hpf5bis/7 and VC2530hpf6bis/8bis for up and down regions of the gene, and primers MV268/269 on pKD4 plasmid for the resistance gene (frt::kan::frt).
pMP7-∆rmf::kan	L045	gibson assembly using primers MV450/451 for the amplification of pMP7 vector, primers VC1484rmf5/7 and VC1484rmf6/8 for up and down regions of the gene, and primers MV268/269 on pKD4 plasmid for the resistance gene (frt::kan::frt).
pMP7-∆crp ::aad7	8348	Baharoglu *et al.*, 2012
pMP7-∆fur::kan	N450	gibson assembly using primers MV450/451 for the amplification of pMP7 vector, primers VC2106fur5/7 and VC2106fur9/8 for up and down regions of the gene, and primers MV268/269 on pKD4 plasmid for the resistance gene (frt::kan::frt).
Primers		
raiAecoRI		ggaattcaccATGAAAATCAACATCACTGGTAA
raiAxba		gctctagaTTATTCCACTTCTTCGCTCAG
hpfeco		ggaattcaccATGCAAATCAACATTCAAGGCC
hpfxba		gctctagaTTAATGACTACTTAGCTTTTCTTT
rmfeco		ggaattcaccATGAAGAGACAAAAGCGTGAT
rmfxba		gctctagaTTATTTGCAGAGACCAGAAAGTTT
ZB47		CCCGTTCCATACAGAAGCTGGGCGAACAAACGATGCTCGC
ZB48		GACATTATTTGCCGACTACCTTGGTGATCTCGCCTTTCACG
ZIP381		GCGAGCATCGTTTGTTCGCCCAGCTTCTGTATGGAACGGGTAAATAGAATGATGGGAGATAGCGC
ZIP382		CGTGAAAGGCGAGATCACCAAGGTAGTCGGCAAATAATGTCAATGCTTTTTCCTCTGTGTCATCCCTTATGG
ZIP383		AACCTATCCAGATACCGAAGCGGC
ZIP384		GTTTTGCAGATAGGATTGCTGAAGC
ZIP93		GTCGAATGCCAAACGAAAGCGGAAAATACC
ZIP94		GCGAGCATCGTTTGTTCGCCCAGCTTCTGTATGGAACGGGTACGGTATTGAAAAAGTGCAGCCTGC
ZIP95		CGTGAAAGGCGAGATCACCAAGGTAGTCGGCAAATAATGTCGCTGGGTATTCCTAAAAATTAAAATATAAAGTCATGC
ZIP96		CACAACAACTCTAGTATCTGGTTTACCCTCG
ZIP97		GGCAGCCTATGCAGGCTGCACTTTTTCAATACCGTCCCGTTCCATACAGAAGCTGGGCGAACAAACGATGCTCGC
ZIP98		ATGACTTTATATTTTAATTTTTAGGAATACCCAGCGACATTATTTGCCGACTACCTTGGTGATCTCGCCTTTCACG
ZIP443		TTATTTGTATAGTTCATCCATGCCATGTGTAATCCCAGC
ZIP444		ATGCGTAAAGGAGAAGAACTTTTCACTGGAGTTGTCC
ZIP446		GGACAACTCCAGTGAAAAGTTCTTCTCCTTTACGCATAATGCTTTTTCCTCTGTGTCATCCCTTATGG
VC2530hpf5bis		CTATTATTTAAACTCTTTCCgccgatggtgctcaacgatg

VC2530hpf7		CTACACAATCGCTCAAGACGTGagactttccttctctagtttagg
VC2530hpf6bis		TACGTAGAATGTATCAGACTcttcacactgcaatagcacg
VC2530hpf8bis		CTAATTCCCATGTCAGCCGTGCGCCAGATCGCCGAAGCTA
VC1484rmf5		CTATTATTTAAACTCTTTCCggcttggttgttagatgatc
VC1484rmf7		CTACACAATCGCTCAAGACGTGagttctgtcctcatacggta
VC1484rmf6		TACGTAGAATGTATCAGACTgttgatgatggatcgcattacc
VC1484rmf8		CTAATTCCCATGTCAGCCGTttcccatacaacaaagcttga
VC2106fur5		CTATTATTTAAACTCTTTCCAAGCGGATGCGAACTTCGC
VC2106fur7		CTACACAATCGCTCAAGACGTGATACTTTCCTGTTGATGTTCTGC
VC2106fur8		CTAATTCCCATGTCAGCCGTGCTCACAAGCCGAAGAAATAA
VC2106fur9		TACGTAGAATGTATCAGACTccacaaatcgatcagtttatgg
ZIP200		TATCAAGCTTATTTGTATAGTTCATCCATGCC
ZIP513		GAG CTG TTG ACA ATT AAT CAT CCG GCT CGT ATA ATG TGT GGA ATT GTG AGC GGA TAA CAA TTT CAC ACA GGA AAC ACA TAT GCG TAA AGG AGA AGA AC